PREPRINTS

OF THE

STEWARD OBSERVATORY

THE UNIVERSITY OF ARIZONA
TUCSON, ARIZONA 85721, U.S.A.

NO. 47

REDSHIFT-MAGNITUDE BANDS, QUASI STELLAR SOURCES, AND SYSTEMS OF REDSHIFT

W.G. Tifft
Steward Observatory
University of Arizona
Tucson, Arizona

Received 1972 August

ABSTRACT

The visibility and character of redshift-magnitude bands in a diagram of general field galaxies compared to specific clusters depends upon the cosmological model. In the normal expanding universe model where galaxies have lives comparable to the age of the universe, no band structure should be visible outside of clusters. Band structure is, however, shown to exist among quasi stellar sources and to show the identical slope and band spacing characteristics as do the galaxies in the Coma cluster. At least 14 bands can be identified forming a convergent band series among QSS emission line objects. The validity of the band phenomenon is tested by power spectrum analysis and shown to be highly significant. The distribution of points about the band structure is Gaussian. Cross projections of the band system are shown to give rise to harmonic periodicities which can explain some or all of the periodicities observed in the z distribution of QSS objects.

The Coma galaxy band system is shown to be a scaled version of the QSS band system. Galaxies appear to occupy a separate band system which is convergent to the start of the QSS system as its series limit. QSS absorption line objects are further shown to apparently form a third independent band system beginning at the high redshift limit of the QSS emission line system.

The band phenomenon is briefly discussed in terms of a model invoking multiple states of matter, rapid galaxy evolution, and possible time evolution of matter observed as a function of lookback time in a singular origin Universe.

INTRODUCTION

The possibility that a non-dynamical correlation exists between the redshift and luminosities of galaxies in a cluster was initially shown by Tifft (1972a) in a paper which shall henceforth be referred to as CI. In CI the galaxies in the Coma cluster were shown to group into bands sloping fainter toward higher redshift in a redshift-magnitude diagram. The slope of the bands is also the direction of maximum morphological separation in the cluster. The Coma cluster bands in this initial study appeared essentially straight and parallel in the m-V_o diagram. The magnitudes utilized, designated V(4.8), were visual nuclear region magnitudes defined as the visual magnitude within a circular zone of 4.8 arc seconds diameter. χ^2 and Student's t testing was used to evaluate the findings.

In a subsequent paper (Tifft, 1973), henceforth referred to as CII, the galaxy sample in the Coma cluster was extended. The band structure was shown to be convergent toward zero redshift and to show possible substructure within the bands which correlates well with both galaxy morphology and the degree of flattening of the galaxies. The convergent redshift-V(R) bands were shown to be nearly straight and parallel in a log(redshift)-V(R) diagram, and appear to be strictly straight and parallel in a log(redshift)-total magnitude diagram. The slope of the total magnitude bands is an important constant which we shall use in this paper and was determined to be

$$a=4.3\pm0.2 \text{ (magnitudes per factor of 2 change in redshift).} \quad (1)$$

The equation of a Coma cluster band was shown to be of the form

$$I_T=K(n)\left(\frac{V_o}{1000}\right)^{-5.7} \quad (2)$$

where I_T is the total apparent visual intensity, V_o is the redshift corrected for local motion, and K(n) is a multivalued "constant" which depends upon the band index n. In logarithmic form this equation is

$$\log \frac{V_o}{1000} = L(n)+0.070m_V, \quad (3)$$

where m_V is the total apparent visual magnitude.

In CII the band pattern was analyzed by power spectrum methods which confirmed and extended the significance level studies of the band pattern in CI. The power spectrum method of Yu and Peebles (1969) as further discussed by Lake and Roeder (1972) was employed. Lake and Roeder (1972) used the method to investigate possible periodicities in the redshift distribution of the QSS, a subject which will also be considered in this paper. In order to apply the power spectrum analysis to the band system, the effect of magntiude is removed by projection to a uniform magnitude (m_V=16.2) along a specified slope. The projection used has the form

$$\log V' = \log V_o - \frac{.301}{s}(m_V - 16.2) \tag{4}$$

where s is the projection slope expressed in magnitudes per factor of 2 in redshift.

The apparent spacing of the Coma cluster bands in CI and CII is not uniform but suggests that they represent part of a sequence converging toward higher redshifts. Since the power spectrum analysis is optimum only for detection of periodic distributions the convergence was nullified by defining a "stretched" form of redshift,

$$V'' = V' + Q(V')^2. \tag{5}$$

In CII power spectra of the Coma cluster galaxy samples were shown to have maximum peak values for small positive Q values.

THE BAND PHENOMENON IN RELATIONSHIP TO COSMOLOGICAL MODELS

Assuming that the band structure phenomenon is a general characteristic of galaxies then any individual group of cluster of galaxies should show the phenomenon independent of the details of the large scale cosmological model. This follows simply from the assumption that all galaxies in a cluster are at the same distance. Studies of clusters other than Coma (1972b and unpublished studies in progress) do appear to indicate that the band phenomenon is a general property of clusters.

If we assume that each galaxy satisfies some absolute magnitude-differential intrinsic redshift law (the band phenomenon) and the ordinary Hubble expansion law, we may represent the redshift of any galaxy as

$$V_o = V_H + V_K. \tag{6}$$

V_H is the Hubble velocity of the galaxy and V_K is the "intrinsic" redshift effect. Peculiar motion is neglected and V_o is the redshift after local motion corrections. From the band convergence phenomenon observed in CII the intrinsic term appears to be of the form

$$V_K = k(n)V_L, \tag{7}$$

where V_L is a "reference" band and $k(n)$ a set of scaling constants dependent upon the band index n. The bands will converge to the Hubble velocity as $V_L \to 0$. In CII the band convergent point for the Coma cluster was shown to be close to zero, hence, $V_H=0$ is a possibility and the entire redshift might be an intrinsic effect,

$$V_o = V_K = k(n)V_L \tag{8}$$

If this were the case the band structure in any cluster should be convergent to zero.

Although the visibility of the band phenomenon in clusters is independent of the cosmological model the character of the structure from cluster to cluster and the character of a composite diagram of several clusters or field galaxies does depend upon the model. Three cases may be distinguished. In the first or "classical" case we have the following assumptions.

1. The properties of matter and energy are fixed at some initial epoch and are not subsequently time dependent (but not necessarily all known!).
2. Galaxies evolve only slowly with time except for perhaps a short initial period.
3. The Universe is expanding in accord with the Hubble law.

To this list we will add the intrinsic differential redshift (band) effect.

4. Each galaxy satisfies some absolute magnitude-differential intrinsic redshift law which is manifest as the convergent band phenomenon.

This model will satisfy nearly all present day observations except the $V_H=0$ possibility in CII. By means of assumption 4, most discordant redshift effects can be explained. Assumption 4 is permitted by the paranthetical qualification of assumption 1.

On the basis of this first model we may make the following predictions relating to the composite log(redshift)-m_V diagram of clusters and field galaxies.

A1. The set of convergent points of the band patterns in clusters should lie along a Hubble line if all clusters are reasonably similar in their properties.

B1. Since the band slope differs from the Hubble slope the general composite log(redshift)-m_V diagram will not show a banded structure.

For the second case we will reject assumption 3 and take $V_H=0$ in accord with the CII suggestion. This model immediately encounters gross difficulties It fails to satisfy either Olber's paradox or the observed Hubble law. The following predictions relating to the composite log(redshift)-m_V diagram of clusters and field galaxies can be made, however.

A2. The set of convergent points of the band patterns in clusters should lie along the origin, $V_o=0$, if all clusters are reasonably similar in their properties.

B2. Since the distance modulii of clusters can differ widely, the general composite log(redshift)-m_V diagram will <u>not</u> show a banded structure.

For the third case we will reject assumption 3 as in the above case and also reject assumptions 2 and perhaps 1. We may now recover both the observed Hubble law and satisfy Olber's paradox by choosing an appropriate intrinsic redshift phenomenon which is time dependent and/or rapid galaxy evolution in time such that redshift and luminosity are a direct function of lookback time (distance). Improbable though this case may seem, it is obviously possible to construct such models and in particular the following conditions can also be satisfied.

A3. The set of convergent points of the band patterns in clusters can lie along the origin, $V_o=0$, if all clusters are reasonably similar in their properties. The banded pattern seen in a particular cluster can depend upon the cluster distance (lookback time).

B3. The composite log(redshift)-m_V diagram can show a banded structure over its entirity.

B3 follows from the fact that galaxies of a particular type (redshift and luminosity) can be seen only at a particular distance (lookback time). Thus, each cluster populates only a specific part of the general intrinsic redshift-magnitude pattern.

A COSMOLOGICAL TEST

The second case discussed in the previous section can be readily ruled out for reasons given there. On the basis of present studies, however, one cannot choose between the first and third cases except by intuitive feelings. From the previous section a formal test is possible by comparing predictions A and B. A failure to find the effects predicted in the third model might not absolutely rule out this type of model since its predictions may not be unique, however, if the predictions of the third model are verified, the first model is in serious jeopardy. We, therefore, frame two fundamental cosmological test questions:

A. Are the convergent points (or asymptotic limits) of the band patterns of all galaxy clusters close to zero?

B. Is the band pattern seen in individual galaxy clusters also visible in a composite redshift-magnitude diagram of unrelated field objects or unrelated clusters?

Test A requires studies of a number of clusters now in progress but not well enough advanced to answer the question. Test B may now be carried out, however, and is one primary objective of this paper. In order to carry out test B a sizeable number of accurate total magnitudes and redshifts of comparable objects over a large part of the sky is required. Many redshifts exist, however, magnitudes of the homogeneity and accuracy required are not available for many galaxies. Since it is generally recognized that the QSS are extragalactic, and since any cosmological phenomenon of the type considered must have an effect on them comparable to if not identical to galaxies, the test was first performed on QSS objects and then related to galaxies. Because of their stellar appearance, photoelectric observations yield directly their total magnitudes, and a sizeable amount of reliable data are available. The question of QSS variablility will be considered later. The test will be more specific than simply detecting a pattern within the QSS redshift-magnitude distribution. The precise hypothesis proposed for the QSS test is as follows:

> Do QSS objects with reliable redshifts and magnitudes show a banded structure in their logz-m diagram with a slope and character of the band spacing identical to the total magnitude bands among galaxies observed in the Coma cluster?

QSS DATA SAMPLE

The primary source employed for data on QSS objects was the catalog by

DeVeny, et. al. (1971). A second short list has been published by Lynds and Wills (1972). One hundred sixty-nine QSS objects on these lists have both z values and V magnitudes not qualified as being uncertain or estimated. One error in the DeVeny, et. al. (1971) list was corrected, 3C380.1 has V=19.44 not 13.44 as quoted. Data on the 169 QSS objects are given in Table 1. Parts of the data are described later in the text. The table is organized into 17 blocks, with objects within each block ordered by z values. An asterisk following a z value indicates the presence of absorption lines in the spectrum.

THE DISTRIBUTION OF z and z'

The band system as recognized in CII in the Coma cluster consists of parallel bands in the log(redshift)-total magnitude diagram with a slope of 4.3 ± 0.2 magnitudes per factor of two in redshift. The first step in the study of the QSS sample was, therefore, to project the $\log z$-m_V diagram of the QSS sample at the predicted slope and several other values for comparison. The projection equation is given in equation 4 with z and z' in place of V_o and V',

$$\log z' = \log z - \frac{.301}{s}(m_V - 16.2). \qquad (9)$$

Figure 1 illustrates the distribution of z' for s=2.5, 4.3, 8.0 and ∞ (z'=z). Absorption line QSS are distinguished from the normal emission line objects. There are no obvious periodicities in the distributions at s=2.5, 8.0, or ∞, however, at the predicted slope of 4.3 a much more distinct clumping is present, especially in the interval z'=0.1 to 1.0 where up to 14 successive clumps may be counted. Beyond z'=1.0 a break in the frequency of emission line (henceforth called QSE) objects occurs and absorption line (henceforth called QSA) objects become more frequent. Table 1 contains the values of z' for each object projected at s=4.28, a value to be derived later in this paper. The objects in table 1 will now be seen to be grouped into related z' groups corresponding to the clumps in figure 1. There are 14 groups by z' plus the few low z' objects and the high z' objects separated as QSE and QSA types.

POWER SPECTRUM ANALYSIS OF z''

In CII the distribution of projected redshifts was studied by power spectrum methods after projection and linearization by equations 4 and 5.

FIGURE 1

The distribution of z' for four different projection slopes, s=2.5, 4.3, 8.0, and ∞ (z'=z). Emission line QSS objects are shown with open circles and QSS objects with absorption lines are shown with filled circles. A periodic clumping of points appears at s=4.3, especially between $0.1<z'<1.0$. No obvious periodicities appear at the other slopes. A break in the QSE frequency for s=4.3 occurs at z'=1.0 above which QSA objects become more prominent.

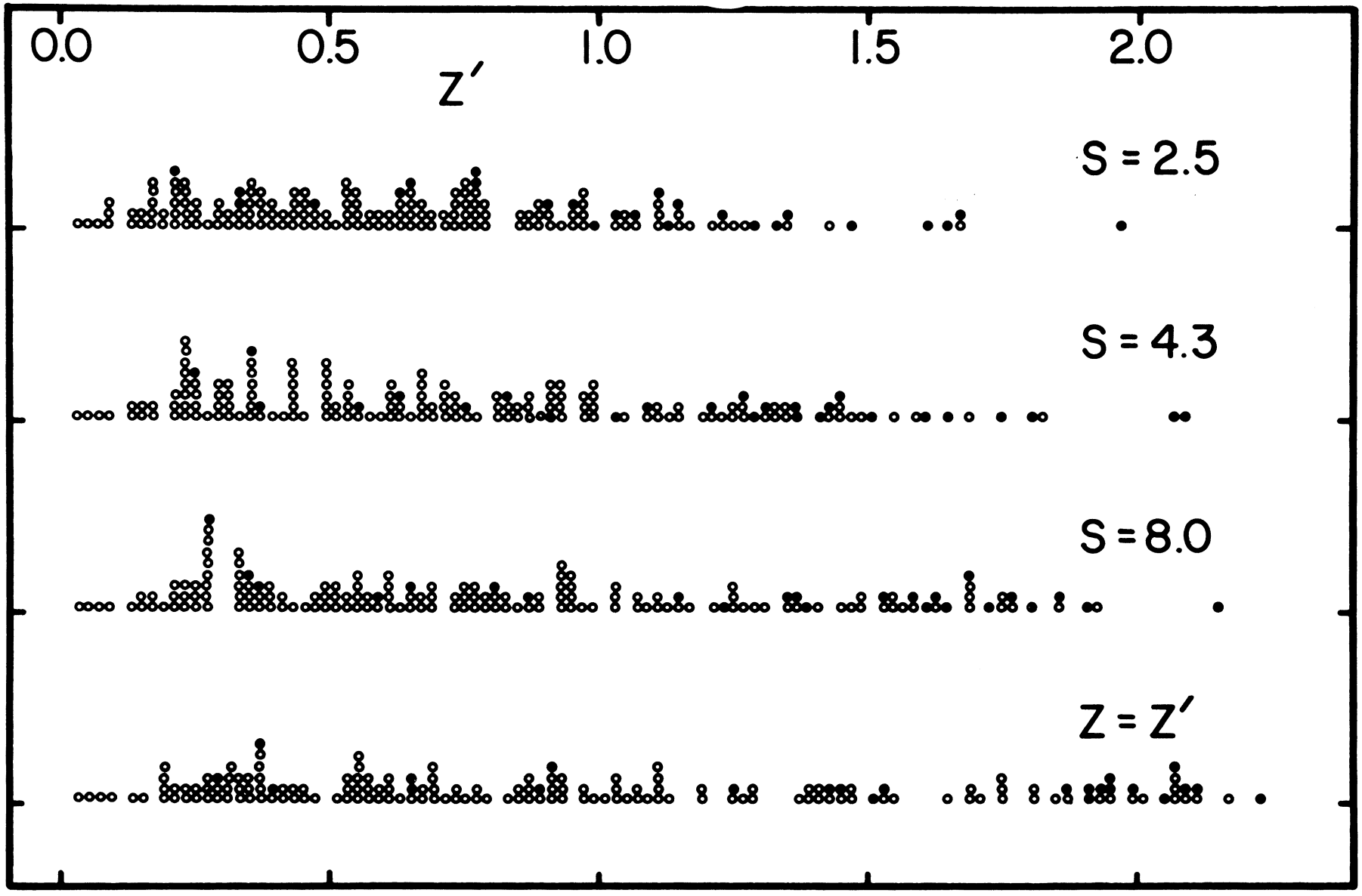
0.0
0.5
1.0
1.5
2.0
Z′
S = 2.5
S = 4.3
S = 8.0
Z = Z′

Table 1

Data on 169 QSS Objects

Identification	V	z	z'
		Low z Group	
B 272	17.25	.036	.030
B 234	17.52	.060	.048
TON 1542	15.30	.064	.074
B 264	16.89	.095	.085
B 154	18.56	.183	.125
BSO 2	18.64	.186	.125
		n=1 Group	
TON 256	15.41	.131	.149
B 340	16.97	.184	.162
B 382	17.55	.194	.156
B 114	17.92	.221	.167
		n=2 Group	
PKS0837-12	15.76	.200	.215
PKS2135-14	15.53	.200	.223
PKS1217+02	16.53	.240	.228
PHL1093	17.07	.258	.224
3C323.1	16.69	.264	.244
B 46	17.83	.271	.208
B 142	17.84	.280	.215
4C9.35	17.24	.298	.252
PHL1194	17.50	.298*	.241
B 337	17.62	.300	.238
4C5.38	17.43	.303	.248
PHL1078	18.25	.308	.221
3C277.1	17.93	.320	.242
B 196	18.28	.323	.231
B 286	18.65	.330	.222
RS 32	18.91	.341	.220
		n=3 Group	
3C273	12.80	.158	.247
PKS1004+13	15.15	.240	.284
PKS1049-09	16.79	.344	.313
PKS1233-24	17.20	.355	.302
PHL1027	17.04	.363	.317
PHL3375	18.02	.390	.290
3C215	18.27	.411	.294
3C47	18.10	.425	.312
B 312	19.08	.450	.282

Table 1 (Continued)

Identification	V	z	z'
	n=4 Group		
3C249.1	15.72	.311	.336
PKS2251+11	15.82	.323	.344
PKS1510-08	16.52	.361*	.343
3C48	16.20	.367	.367
PKS2145+06	16.47	.367	.351
PKS1229-02	16.75	.388*	.355
4C10.30	17.10	.420	.363
4C21.35	17.50	.435	.352
5C02.10	18.00	.478	.357
3C275.1	19.00	.557	.354
	n=5 Group		
TON 202	15.68	.366	.398
3C351	15.28	.371	.431
PHL658	16.40	.450	.436
3C279	17.75	.536	.417
4C10.33	17.49	.540	.438
3C147	17.80	.545	.421
PKS1136-13	17.80	.554	.428
PKS1634+26	17.75	.561	.436
3C261	18.24	.614	.441
	n=6 Group		
PKS1327-21	16.74	.528	.484
PKS0403-13	17.17	.571	.488
PKS0405-12	17.07	.574	.499
MSH13-011	17.68	.625	.492
3C207	18.15	.684	.499
B 246	18.18	.690	.501
3C138	18.84	.759	.495
	n=7 Group		
PKS2128-12	15.99	.501	.518
3C232	15.78	.530	.567
3C334	16.41	.555	.536
3C281	17.02	.599	.525
PKS0155-10	17.09	.616	.533
PKS0932+02	17.39	.659*	.543
4C39.25	17.86	.698	.533
3C254	17.98	.734	.550

Table 1 (Continued)

Identification	V	z	z'
	n=8 Group		
3C345	15.96	.594	.618
PKS0349-14	16.22	.614	.612
3C380	16.81	.691	.626
PHL923	17.33	.717	.597
B 471	17.66	.774	.611
4C09.37	17.86	.786	.601
3C2	19.35	1.037	.623
	n=9 Group		
4C16.30	15.70	.634	.687
3C263	16.32	.652*	.639
3C57	16.40	.680	.658
4C19.34	17.49	.828	.672
3C196	17.79	.871	.673
4C20.33	17.86	.871	.666
PKS0922+14	17.96	.895	.673
4C37.24	18.11	.914	.671
B 330	18.01	.920	.686
	n=10 Group		
PKS2344+09	15.97	.677	.703
PKS1354+19	16.02	.720	.741
3C175	16.60	.768	.720
3C286	17.25	.846	.714
PKS1317-00	17.32	.890*	.742
PKS0957+00	17.57	.907	.727
3C336	17.47	.927	.755
3C288.1	18.12	.961	.704
4C05.46	18.94	1.115	.715
	n=11 Group		
PKS1252+11	16.64	.870	.810
3C309.1	16.78	.905*	.824
MSH14-121	17.37	.938	.776
4C10.34	18.08	1.088	.802
3C204	18.21	1.112	.803
	n=12 Group		
PKS2216-03	16.38	.901	.875
CTD 141	17.30	1.015	.849
3C245	17.29	1.029	.862
CTA 102	17.33	1.037	.864
3C287	17.67	1.055	.831
3C186	17.60	1.063	.847
4C13.46	18.09	1.137	.837

Table 1 (Continued)

Identification	V	z	z'
	n=13 Group		
3C454.3	15.76	.859	.922
3C94	16.49	.962	.918
PKS2115-30	16.47	.980	.938
3C208	17.42	1.110	.911
B 228	17.83	1.194	.917
PKS1454-06	18.00	1.249	.933
B 288	18.39	1.293	.907
3C181	18.92	1.382	.890
4C18.34	18.74	1.401	.929
	n=14 Group		
PKS0122-00	16.70	1.070	.987
PKS1055+20	17.07	1.110	.964
RS 13	17.94	1.287	.971
3C268.4	18.42	1.400	.977
3C446	18.39	1.404	.985
4C31.38	18.96	1.557	.996
3C280.1	19.44	1.659	.982
	High z QSE Group		
PKS1127-14	16.90	1.187	1.060
4C06.41	16.81	1.270	1.151
B 201	16.79	1.375	1.250
B 86	17.58	1.431	1.144
4C17.46	17.90	1.449	1.100
A00952+17	17.23	1.472	1.246
PHL3632	18.15	1.479	1.078
B 185	18.12	1.530	1.121
4C11.32	19.06	1.754	1.104
4C19.31	17.73	1.691	1.320
4C06.40	18.30	1.699	1.209
PKS0922+005	18.07	1.720	1.271
BSO 8	17.43	1.750	1.434
3C454	18.40	1.757	1.230
3C432	17.96	1.805	1.357
PKS2354+14	18.18	1.810	1.313
PHL3424	18.25	1.847	1.325
4C13.39	17.80	1.875	1.447
4C 29.50	19.14	1.927	1.197
BSO 6	17.87	1.956	1.492
PKS1148-00	17.60	1.982	1.580
3C9	18.21	2.012	1.453
PHL1305	16.96	2.064	1.825
B 19	17.94	2.065	1.558
B 189	19.22	2.075	1.272
B 360	17.56	2.090	1.677
PKS0106+01	18.39	2.107	1.478
4C11.45	19.13	2.171	1.351

Table 1 (Continued)

Identification	V	z	z'
	High z QSA Group		
BSO 1	16.98	1.241*	1.094
PHL1377	16.49	1.434*	1.368
3C298	16.79	1.439*	1.308
3C270.1	18.61	1.519*	1.028
3C205	17.62	1.534*	1.219
B 194	17.96	1.864*	1.402
RS 23	18.74	1.908*	1.265
PHL1222	17.63	1.910*	1.515
PHL938	17.16	1.930*	1.652
3C191	18.40	1.952*	1.367
PKS0119-04	16.88	1.955*	1.751
PHL1127	18.29	1.990*	1.419
TON 1530	17.00	2.051*	1.802
PKS0229+13	17.71	2.065*	1.617
BSO 11	18.41	2.084*	1.457
PKS1116+12	19.25	2.118*	1.292
PKS0237-23	16.63	2.224*	2.074
PHL957	16.60	2.720*	2.549
4C05.34	18.16	2.877*	2.095

The equivalent equations for the QSS sample are equation 8 for projection and

$$z'' = z' + Q(z')^2 \qquad (10)$$

for linearization. Initially to avoid bias on choice of parameters we shall consider Q=0 and test at the predicted slope s=a determined from the Coma cluster, hence, no free parameters enter into the initial power spectrum calculations. The first power spectrum calculations were done using only the 143 QSE objects, however, it will be shown later that adding the 26 QSA objects makes no important difference.

Figure 2 is a plot of the 143 QSE power spectrum for Q=0, s=4.3. The spectrum shows a peak of 9.0 at a wavelength of 0.0635. According to the probability table for peaks of a given power level given in CII, this peak is significant below the 0.02 level and confirms the subjective impression of the previous section that a basic periodicity is present at s=4.3.

From CII it is known that small positive Q values linearize the apparent band projection sequence, hence, increase the peak in the power spectrum. Power spectra were, therefore, next calculated for the 143 QSE sample for a series of positive Q values. Figure 3 shows the effect on the dominant power spectrum peak. Near Q=0.08 the peak rises to no less than 12.4. The effect of increasing Q in adjusting the phasing of the z' concentrations first produces a minimum power near Q=0.025 where maximum interference of the clumping apparently occurs, and then produces a very sharply peaked spectrum when the total distribution is phased. The probability of finding a random peak in excess of 12 is less than 10^{-3}.

Having established the presence of a highly significant periodicity in the QSE log(redshift)-magnitude distribution at the predicted slope and with the predicted convergent character, the region around the peak was mapped to find the absolute peak. Table 2 contains a tabulation of peak power values for a range of s and Q. The highest peak lies close to s=4.25, Q=0.073 well within the range of predicted slope uncertainty. Figure 4 is an illustration of the power spectrum for the highest peak.

The peak power distribution in table 2 is somewhat irregular but consistently very high. The source of the irregularity is believed to be the higher z'' points which may not be as well phased. This effect was investigated by adding the 26 QSA objects to the 143 QSE sample; most of the QSA objects have high redshifts. Table 3 contains the peak power spectrum

FIGURE 2

The power spectrum of z' for 143 QSE objects projected at s=4.3 which is the slope of the total magnitude bands in the Coma cluster. The conversion between frequency, n, and wavelength, λ, is shown. The power spectrum peak near n=28 is significant at the 0.02 level; the 0.05 significance level is indicated. This peak confirms the impression of periodicity seen in figure 1 at s=4.3.

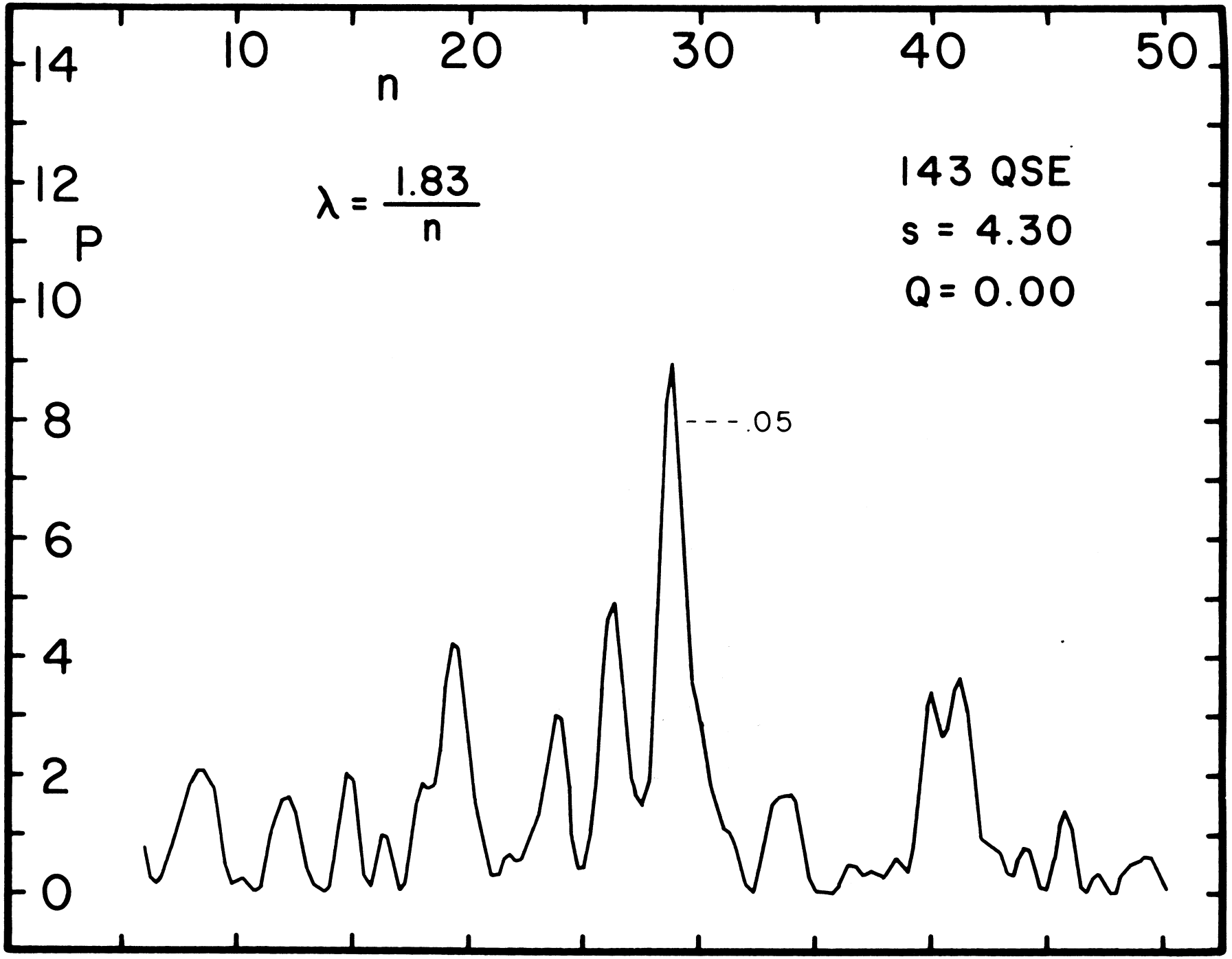
14
10
20
30
40
50
n
12
P
10
8
6
4
2
0
$\lambda = \frac{1.83}{n}$
143 QSE
s = 4.30
Q = 0.00
---.05

FIGURE 3

The effect of "linearization" of the z' distribution for the 143 QSE sample projected at s=4.3. The power contained in various frequencies is plotted against the quadratic stretching factor Q from equation 10. Maximum interference of the z'' clumping occurs near Q=0.025; as $Q \rightarrow 0.08$, the total distribution is phased and a very strong peak occurs in the power spectrum. The distribution of clumps (band projections) in z' apparently forms a smoothly convergent series which the factor Q linearizes.

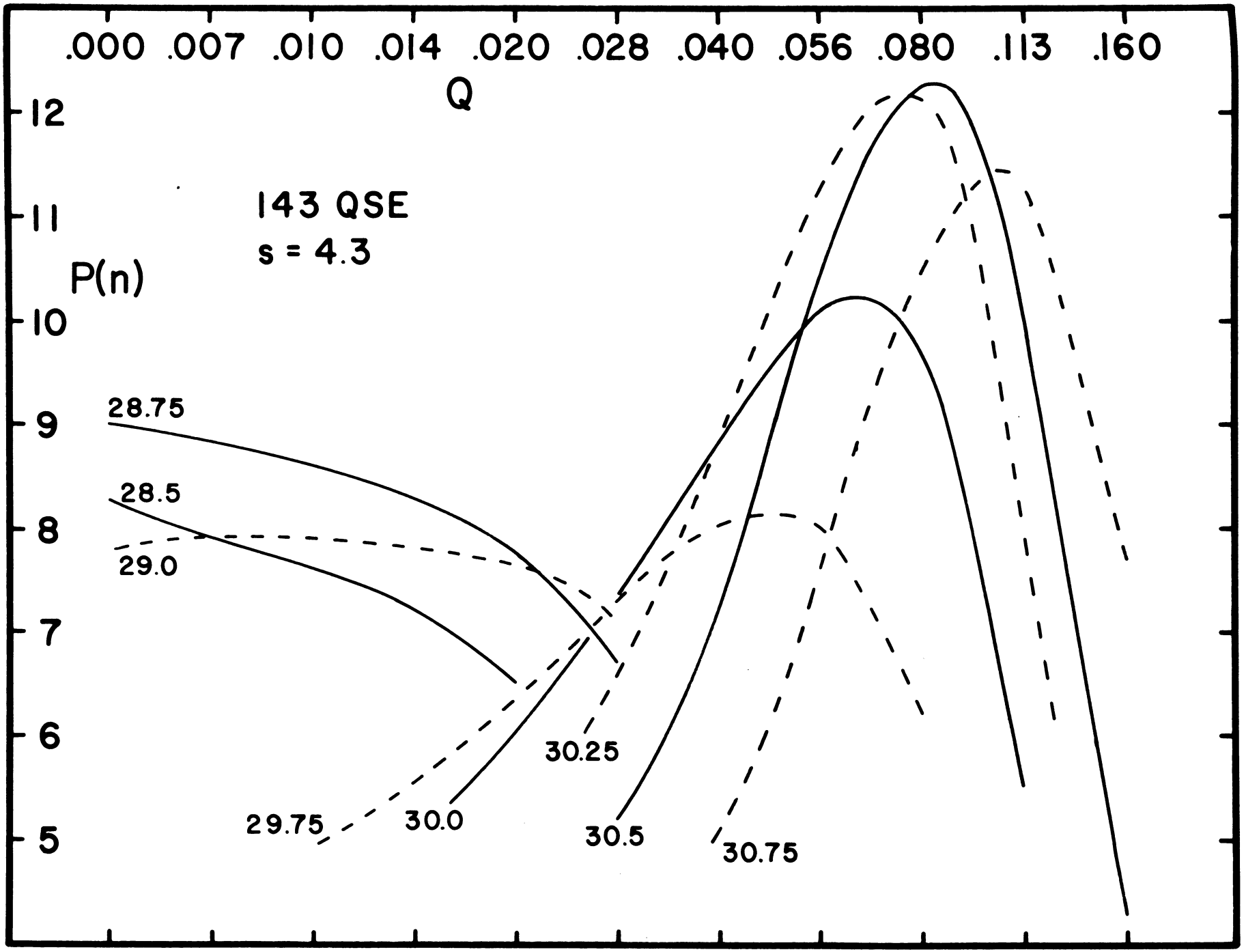
.000 .007 .010 .014 .020 .028 .040 .056 .080 .113 .160
Q
12
11
10
9
8
7
6
5
P(n)
143 QSE
s = 4.3
28.75
28.5
29.0
29.75
30.0
30.25
30.5
30.75

Table 2

Peak Power for 143 QSE Sample

Q \ s	4.0	4.1	4.15	4.2	4.25	4.3	4.35	4.4	4.6
.0000	6.8	8.0		8.6		9.0		9.0	7.1
.0071	6.6	7.8		8.4		8.8		8.8	6.9
.0100	6.3			8.3		8.6		8.7	6.7
.0141						8.3			
.0200	7.2			7.4		7.7		7	5.8
.0283						7.3			
.0400	9.8	9.6	9.2	9.2	9.1	8.8	8.8	8.5	7.1
.0566	10.5	11.4	11.6	11.4	11.5	11.3	10.8	10.1	
.0600			11.8	12.0	11.9	11.5	11.2		
.0660			11.9	12.4	12.4	12.1	11.6		
.0726			12.0	12.5	12.7	12.4	11.9		
.0800	10.1	11.1	11.8	12.4	12.6	12.3	11.9	11.3	7.5
.0878			11.5	12.0	12.1	12.2	11.8		
.0966			11.4	11.6	11.8	11.6	11.2		
.1063			12.0	12.1	11.8	11.4	10.7		
.1130	10.6	11.8	12.1	12.4	12.3	11.7	11.0	10.0	
.1169			12.4	12.5	12.4	12.0	11.2		
.1600	7.3	8.5	9.6	10.3	10.5	10.3	9.6	8.8	9.0

FIGURE 4

The power spectrum of z'' for 143 QSE objects projected at s=4.25 and linearized with Q=0.073. This is the optimum spectrum for the 143 QSE sample. The power spectrum peak near n=30 is significant at below the 0.001 level; a scale of probabilities is indicated. The conversion between frequency, n, and wavelength, λ, is indicated. The frequency of the primary peak is slightly greater than the peak in figure 2 because of the effect of Q on the z' distribution shape and upper limit.

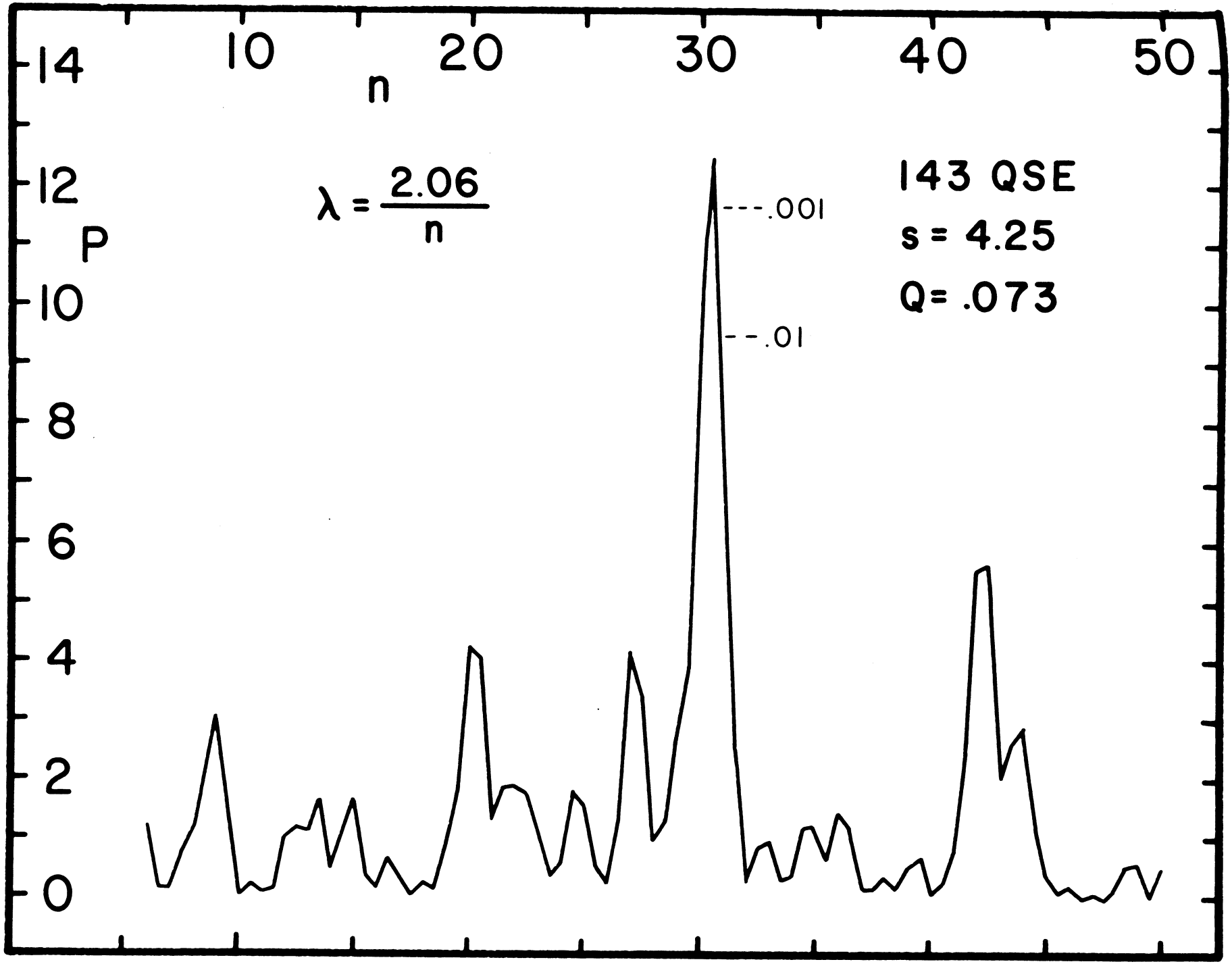
14
10
n
20
30
40
50
12
P
10
8
6
4
2
0
$\lambda = \frac{2.06}{n}$
---.001
--.01
143 QSE
s = 4.25
Q= .073

Table 3

143 QSE + 26 QSA Peak Power Values

Q \ s	4.15	4.2	4.25	4.3	4.35
.06	11.9	11.1	10.1	9.6	9.9
.066	12.7	12.1	11.3	10.3	9.3
.0726	12.5	12.3	11.7	10.9	9.9
.0799	12.2	11.8	11.2	10.6	9.8
.0878	12.0	11.8	11.5	11.2	11.0
.0966	10.6	11.0	11.3	11.6	11.7
.1063	11.5	12.0	12.1	11.6	11.0
.1169	11.2	12.1	12.4	12.4	12.0
.1286	10.6	11.3	11.8	12.0	11.8
.1415	11.1	11.7	12.5	13.2	12.9
.1556	12.9	13.4	13.0	12.2	11.8

values for the total 169 QSS sample calculated in the vicinity of the previously defined maximum. The power remains consistently very high, however, the distribution becomes even more irregular. We infer that high z' objects while consistent with the basic hypothesis of the significance of the slope a=4.3 are not especially well phased by the simple single parameter equation employed.

To test this hypothesis further, power spectrum analysis was carried out for a sample excluding high z' objects. Objects with z' greater than 1.0 were excluded as were the six lowest z' objects so that the periodicity in just the well populated portion of figure 1 could be evaluated. This sample contained 109 QSE and 7 QSA which are the objects in the 14 blocks of table 1 designated as n=1 to 14. Table 4 contains the power spectrum peak values in the restricted system. The peak power exceeds 14 and is now well defined without the irregularity present with the larger samples. It is concluded that the high z' objects were indeed detracting slightly from the peak power. The optimum power peak appears to lie close to s=4.28, Q=0.078. s=4.28 is the value used to generate z' in table 1. Figure 5 is the final power spectrum at the restricted "14-band" system peak. This peak has a probability of less than 10^{-4} of occuring at random.

At this point we may state with a high degree of confidence that the QSS objects in at least the restricted range $0.14<z'<1.0$ show a banded pattern arranged in a convergent series. The potential cosmological significance of this has already been mentioned; the answer to cosmological test B is apparently affirmative. In the subsequent sections of this paper some of the peoperties of the band system will be considered including its relationship to galaxies.

THE QSE BAND SYSTEM

Figure 6 is a logz-m_V plot of the 116 objects in the restricted "14-band" QSS sample. This distribution is dominated by QSE objects and will be called the QSE band system. What occurs at the high and low z boundaries of the QSE band system will be considered further later. In this section, some of the detailed properties of this system alone will be considered. Table 5 contains the mean z' values and band populations k of the QSE system as well as other quantities to be discussed below.

Although the power spectrum analysis was used to demonstrate the existence of the QSE band system, a more useful description of the system

Table 4

109 QSE + 9 QSA in 14-Band System

Q \ s	4.05	4.10	4.15	4.20	4.25	4.30	4.35	4.40	4.45	4.50
.0600	11.4	12.2	13.0	13.7	14.1	14.0	13.6	13.2	12.7	11.8
.0660	11.4	12.3	13.1	13.7	14.2	14.2	13.7	13.3	12.7	11.9
.0726	11.5	12.4	13.2	13.7	14.2	14.3	13.9	13.2	12.8	12.0
.0799	11.5	12.5	13.2	13.7	14.2	14.3	14.0	13.2	12.8	12.0
.0878	11.5	12.5	13.1	13.6	14.2	14.3	14.0	13.2	12.7	12.0
.0966	11.6	12.4	12.9	13.5	14.0	14.2	14.0	13.2	12.6	12.0
.1063	11.6	12.3	12.8	13.5	13.8	14.0	13.8	13.2	12.4	11.9
.1169	11.5	12.1	12.8	13.5	13.6	13.7	13.6	13.0	12.2	11.7

FIGURE 5

The power spectrum of z'' for the restricted 116 QSS sample with $0.14<z'<1.0$ at $s=4.28$, $Q=0.078$ which is optimum for the sample. The main peak is significant below the 10^{-4} level; a probability scale is shown. The conversion between frequency, n, and wavelength, λ, is indicated. The frequency of the primary peak differs from figures 2 and 4 because of the slightly different s and Q values and because the higher z objects which fixed the range of z' for the larger sample have been removed. The increase of the peak value over that in figure 4 indicates that the high z objects were not well phased with the restricted group, hence, do not follow the same convergent series pattern.

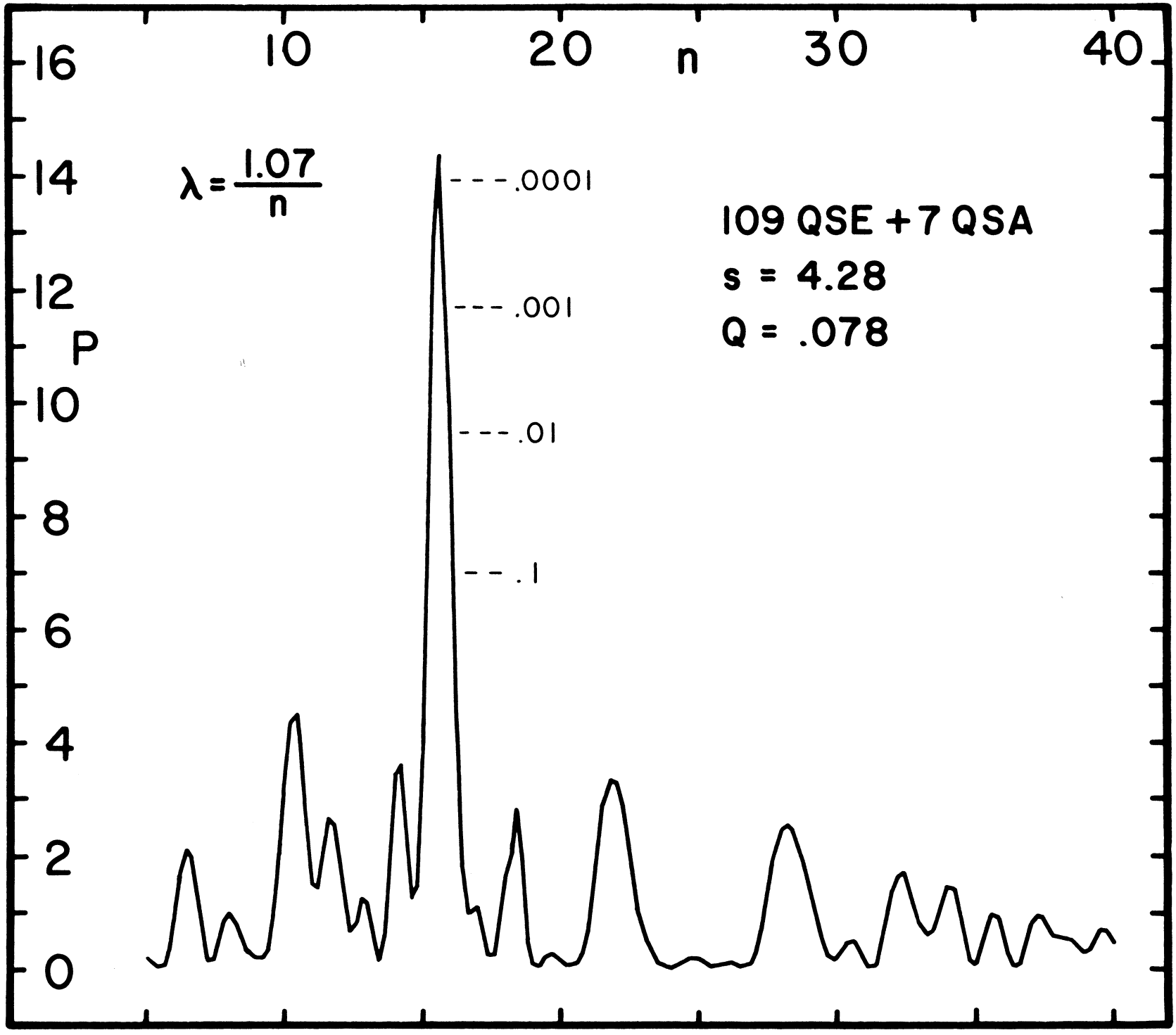
16
10
20
n
30
40
14
12
P
10
8
6
4
2
0
$\lambda = \frac{1.07}{n}$
---.0001
---.001
---.01
--.1
109 QSE + 7 QSA
s = 4.28
Q = .078

Table 5

Properties of the QSE Band System

n	$\bar{z}'$	k	J(n)	z' Calc	z'' Calc	ϕ Calc	σ_ϕ	σ_V
1	.159	4	-1.9266	.163	.165	2.40	.12	.33
2	.229	16	-1.7810	.228	.232	3.38	.19	.35
3	.296	9	-1.6727	.293	.300	4.35	.23	.31
4	.352	10	-1.5866	.357	.367	5.33	.16	.18
5	.427	9	-1.5152	.421	.435	6.32	.22	.21
6	.494	7	-1.4543	.484	.502	7.30	.18	.14
7	.538	8	-1.4012	.547	.571	8.29	.27	.19
8	.613	7	-1.3540	.610	.639	9.29	.16	.10
9	.669	9	-1.3119	.672	.707	10.28	.22	.13
10	.725	9	-1.2736	.734	.776	11.28	.32	.17
11	.803	5	-1.2387	.800	.845	12.28	.30	.13
12	.852	7	-1.2065	.857	.914	13.28	.25	.11
13	.918	9	-1.1768	.917	.983	14.29	.23	.10
14	.980	7	-1.1491	.978	1.052	15.29	.15	.06
1-4		39					.19	.30
5-8		31					.21	.17
9-14		46					.25	.12
1-14		116					.22	

FIGURE 6

The QSE band system. The 14 bands form the smoothly convergent series which produced the power spectrum shown in figure 5. The points associated with alternate bands are shown with alternate symbols except for 7 QSA objects marked with X symbols. The upper envelope is a Hubble line of standard slope 5. Two features used for fitting are shown dashed and are believed to represent physical grouping equivalent to the possible spin groups in the Coma cluster band structure.

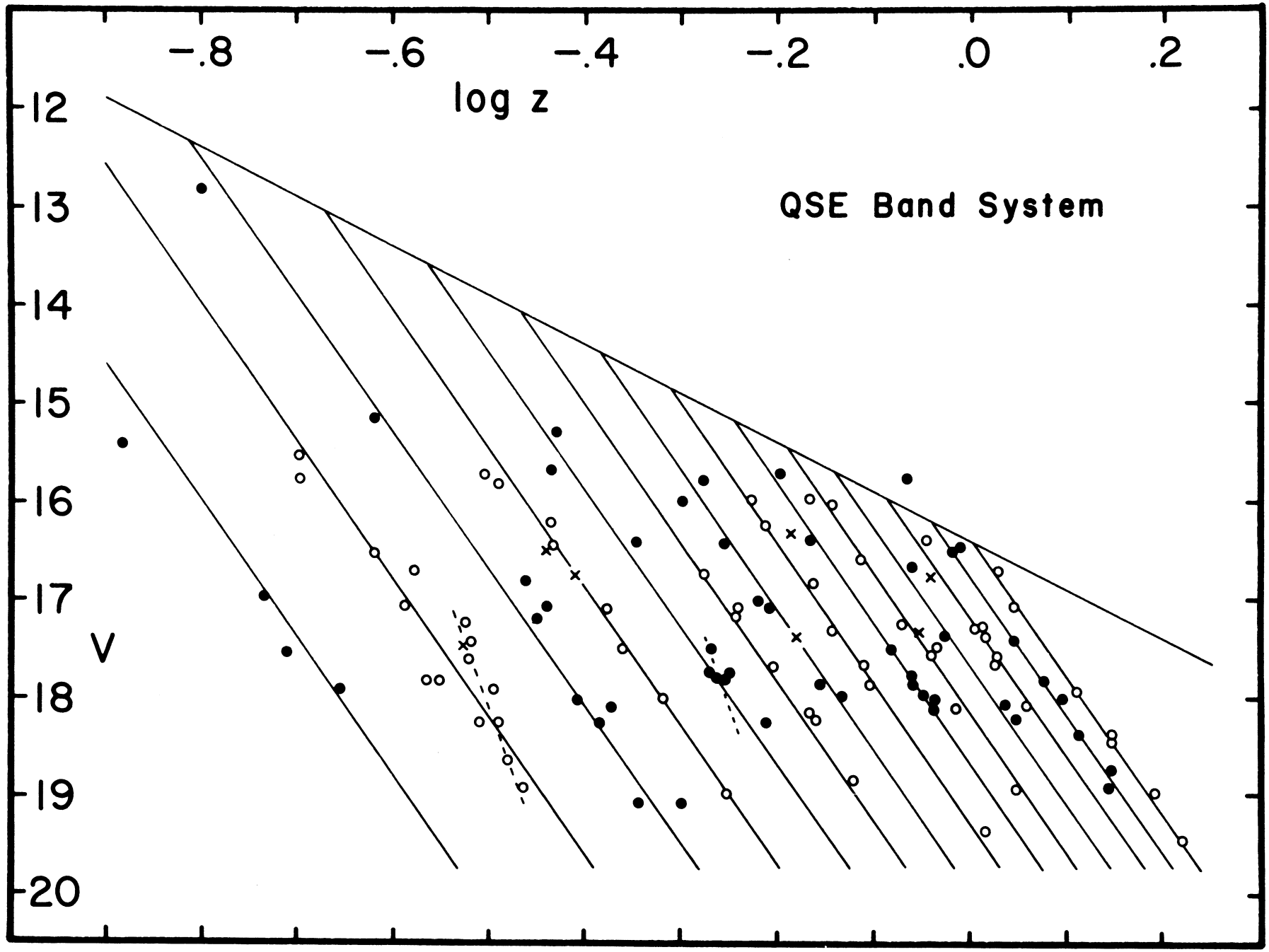
−.8
−.6
−.4
−.2
.0
.2
log z
12
13
14
15
16
17
18
19
20
V
QSE Band System

can be given by fitting a second order polynomial directly through the mean z' values of table 5. Each band can be characterized with a serial band number n in order of increasing redshift such that

$$\overline{z}' = c + dn + en^2. \tag{11}$$

The least squares fit to the 14 bands gives

$$\overline{z}' = 0.0978 + 0.0656n - 0.000195n^2 = j(n) \tag{12}$$

Substituting in equation 9 we may now write the equation of the entire band system directly relating z and m_V. Defining

$$J(n) = \log\left[j(n)10^{-\frac{0.301(16.2)}{4.28}}\right] \tag{13}$$

we find

$$\log z = J(n) + 0.07033m_V, \tag{14}$$

$$m_V = 14.22\left[\log z - J(n)\right] . \tag{15}$$

A tabulation of J(n) is included in table 5 along with the calculated z' and z'' values for the band centers.

Since equation 11 has more degrees of freedom than equation 10, the fit to the band system is slightly different. This is shown in table 5 where the phase

$$\phi = \frac{z''}{T} \tag{16}$$

of the calculated band centers is tabulated. T is the basic periodicity in the power spectrum analysis. For s=4.28, Q=0.078, T=0.0688. The phase of the calculated band centers shows a slight drift especially for low n.

Using the values of ϕ for individual QSS we can examine the distribution of points about the band centers. If the band phenomenon is a physical reality, this phase distribution should have a reasonable form, presumably Gaussian, as was found for galaxies in CI. Figure 7 illustrates the phase distribution of z'' about the calculated band centers. The distribution is

FIGURE 7

The upper part of the figure contains the phase distribution ϕ of the 116 QSE band system objects about the band centers defined by equation 12. The distribution is shown over two cycles to make the modulation clearly visible. The distribution is Gaussian with σ=0.22, or less than 1/4 of the band spacing. In the lower part of the figure the V magnitude residuals about the band centers are shown for three ranges of band number n. The approximate spacing to adjacent bands for each interval is shown with dashed lines. The V dispersion decreases smoothly with n while the phase dispersion remains essentially constant.

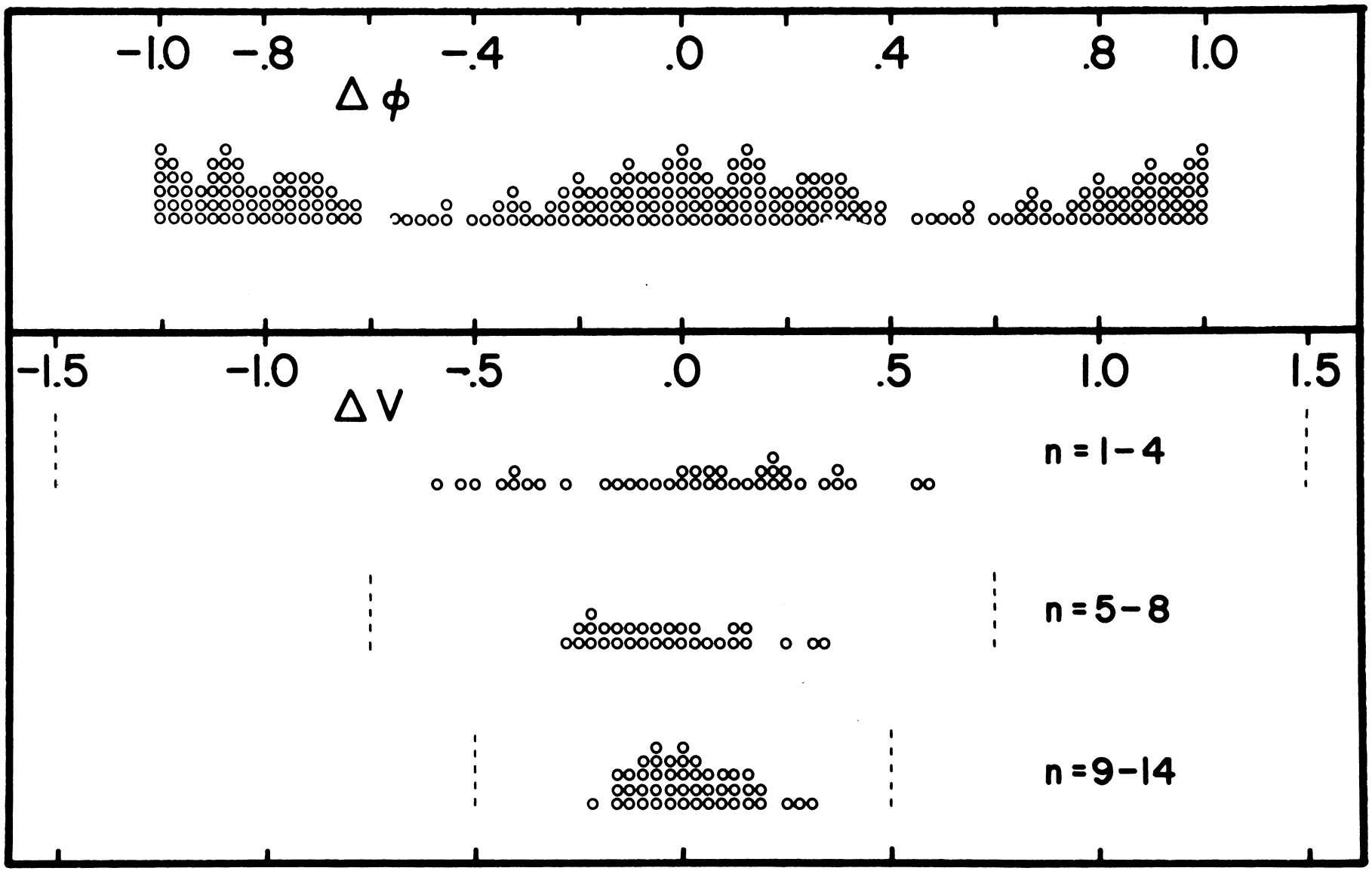
-1.0
-.8
-.4
.0
.4
.8
1.0
Δ φ
-1.5
-1.0
-.5
.0
.5
1.0
1.5
Δ V
n = 1-4
n = 5-8
n = 9-14

effectively Gaussian with a dispersion of 0.22 which is less than one quarter of the z'' band spacing T. Table 5 contains the phase dispersion σ_ϕ about each band center. The phase dispersion is apparently nearly independent of n. It may increase slightly but much less than the band spacing decreases with n.

Given equations 14 and 15, we may calculate predicted z and m_V values for any QSS in the QSE band system and examine the distribution of z or m_V residuals. There are at least seven sources of deviation from the calculated band centers.

1. Intrinsic width of the bands.
2. Variation in object distance.
3. Variability in luminosity.
4. Galactic and intergalactic absorption.
5. Observational errors.
6. True velocity dispersion.
7. Band fitting uncertainties.

The first effect is unknown and relates to the structure of the bands, including substructure such as discussed in CII for the Coma galaxy band system. The sixth effect is probably negligable; the second through fifth effects are probably the dominant sources of scatter. The second through fourth will effect magnitudes only and the fifth is probably of importante only for magnitudes. It is, therefore, likely that most of the scatter other than intrinsic or from fitting arises from magnitude uncertainty. Table 5 contains the magnitude dispersion σ_V about each band. Figure 7 contains plots of the magnitude residuals from the band centers for bands 1-4, 5-8, and 9-14. There is a smooth decrease in the dispersion with n. This is consistent with the essentially constant z'' phase dispersion which requires a decreasing spread in z or m_V along the convergent band series. Of the various sources of magnitude dispersion, only effect 2 and possibly 1 on the above list are good candidates to explain the decreasing dispersion with n. Distant objects will show less magnitude dispersion if they occupy the same lookback time interval (distance interval) as nearby objects.

PERIODICITIES IN z

Various studies of the distribution of z of QSS and related objects have been made. The most recent study by Lake and Roeder (1972) summarizes most earlier work. Various periodicities of marginal significance have been

reported at or near wavelengths of 0.17, .07-.06, 0.026, and 0.018. None of these periodicities in z approach the significance level of the periodicity in z" discussed in the first part of this paper. It is of interest to ask, however, how the z periodicities arise, and if they are related in any way to the band phenomenon. In figure 8 a schematic diagram of the QSE band system is presented. When projected in direction A, the strong basic periodicity of the band system is revealed as previously discussed. In direction A the upper half of each band is in phase with the lower half and we have complete reinforcement. At slopes B or C the bands, simply represented as upper and lower portions, have different numbers of cycles in a given interval, therefore, a sort of interference phenomenon occurs in projection. Various degrees of partial phasing can be expected when the ratio of the band spacings in the upper vs lower parts of the bands have a simple relationship to each other, for example 3/4, 2/1, 7/5, etc. To test this concept, and possibly account for the observed periodicities in z, power spectra were calculated for a wide range of projection slopes. Since we wish to approach $s=\infty$ in some reasonable way, a projection angle τ was defined by

$$\tan\tau = \frac{s}{2.4} , \qquad (17)$$

where the factor 2.4 is an arbitrary factor for scaling convenience. Power spectrum computations were then carried out in 1^{o} steps of τ from 30^{o} (s=1.39) to 90^{o} ($s=\infty$). In order to check fully for all important periodicities, the range was studied for three values of Q, 0.00, 0.02, and 0.08. The original 143 QSE sample was used so small changes will occur if the complete or restricted samples are used, however, it seems unlikely that any important difference would be found.

In a normal power spectrum analysis of a random distribution of points, the number of peaks of various power levels should follow statistical distributions as discussed by Lake and Roeder (1972). This was the approach used to evaluate the primary periodicity in z' identified in the first part of this paper. Once it is recognized, however, that the distribution being tested is not a random one, even very small peaks in the power spectrum take on a significance. For example, at some cross projection in the band system there may be only a weak reinforcement of a particular frequency related to the band structure. A large number of such related peaks obviously has significance even though the individual peaks are very low in power.

FIGURE 8

A schematic diagram of a band system showing how projection at various slopes produces interference effects. In direction A full reinforcement occurs while in direction B or C various degrees of constructive or destructive interference are possible. Such effects are believed to account for some or all of the periodicities which have been observed in the z distribution of QSS objects.

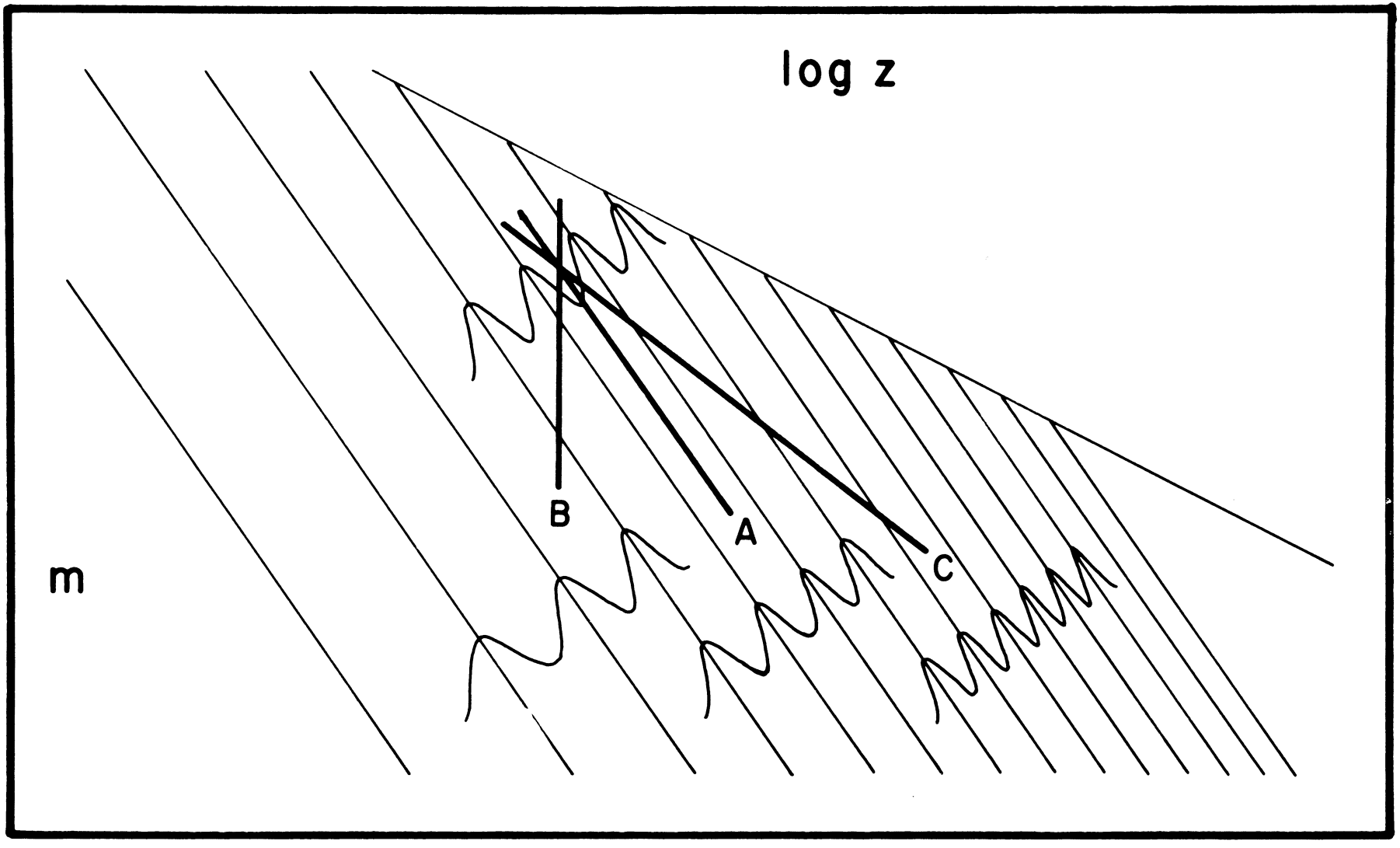
log z
m
B
A
C

Figure 9 is a plot of the wavelength of peaks in the power spectrum of z'' against projection angle τ for Q=0 and wavelength of $0.23 \gtrsim \lambda \gtrsim 0.1$. Higher frequencies, which are somewhat more complex will be considered later. All power spectrum values larger than 0.5 are indicated. A sloping line labeled 1 appears in the right hand part of the figure. It is near this line that peaks in the power spectrum directly related to the primary peak fall. Various harmonic multiples of this locus of basic wavelengths lie to the left as indicated. One can immediately see that many small peaks lie along the basic "harmonic" lines, notably 4/3, 3/2, 2, 5/2, 3, and 7/2. The diagram obviously does not show random scattered peaks but is in fact sort of an interferogram of the band pattern. If we examine the character of the diagram at $\tau=90^{o}$ which corresponds to the distribution of z, we can identify the wavelength 0.17 with the second harmonic line. This is one of the characteristic wavelengths which has been noted in the distribution of QSS redshifts.

In figure 10 we examine the high frequency end of the λ-τ diagram for Q=0. Because of the rapid fluctuations and many harmonics that appear, the diagram is restricted to peaks of power 3.5 or higher. Essentially all the common expected harmonic or subharmonic multiples of the primary wavelength are present. At $\tau=90^{o}$ we note that the 3/4 subharmonic line terminates close to 0.07 and the 2/3 line near 0.06 which are near the most common periodicities found in analysis of QSS z distributions. The periodicities of 0.026 and 0.018 may represent the 1/3 and 1/4 or 1/5 subharmonics, however, this part of the power spectrum has not been well studied. It should also be noted that no exact analytic form of the harmonic lines in these figures has been derived. They have been drawn as straight lines which well represent the low frequencies in figure 9, hence, their $\tau=90^{o}$ intercepts are only approximate.

Figures 11 and 12 are identical to figure 10 excepting for Q=0.02 and 0.08 respectively. These figures show how the various degrees of linearization interact with the projection slope to vary the power distribution.

One final point concerns the clustering of moderately powerful peaks near $\tau=75^{o}$ and 1/2 to 1/3 the primary wavelength. These points may be harmonic interaction, however, another explanation is possible. $\tau=75^{o}$ is close to s=8.5 which is essentially the slope of the "spin group" substructure observed in the Coma cluster in CII. Both the slope and characteristic spacing suggest that similar substructure could be present in the QSE band system and be exciting the peaks in the power spectrum.

FIGURE 9

The wavelength, λ, of points in the z'' power spectrum with P>0.5, as a function of projection angle, τ, for the 143 QSE sample at Q=0.00. Only the longer wavelengths are shown; all power spectrum points in excess of 0.5 are plotted with spot size proportional to power level. The points group about lines which are simple multiples of the primary band pattern frequency. The 0.17 periodicity which has been observed in QSS z distributions can be identified with the X2 multiple of the primary band wavelength at $\tau=90^{o}$.

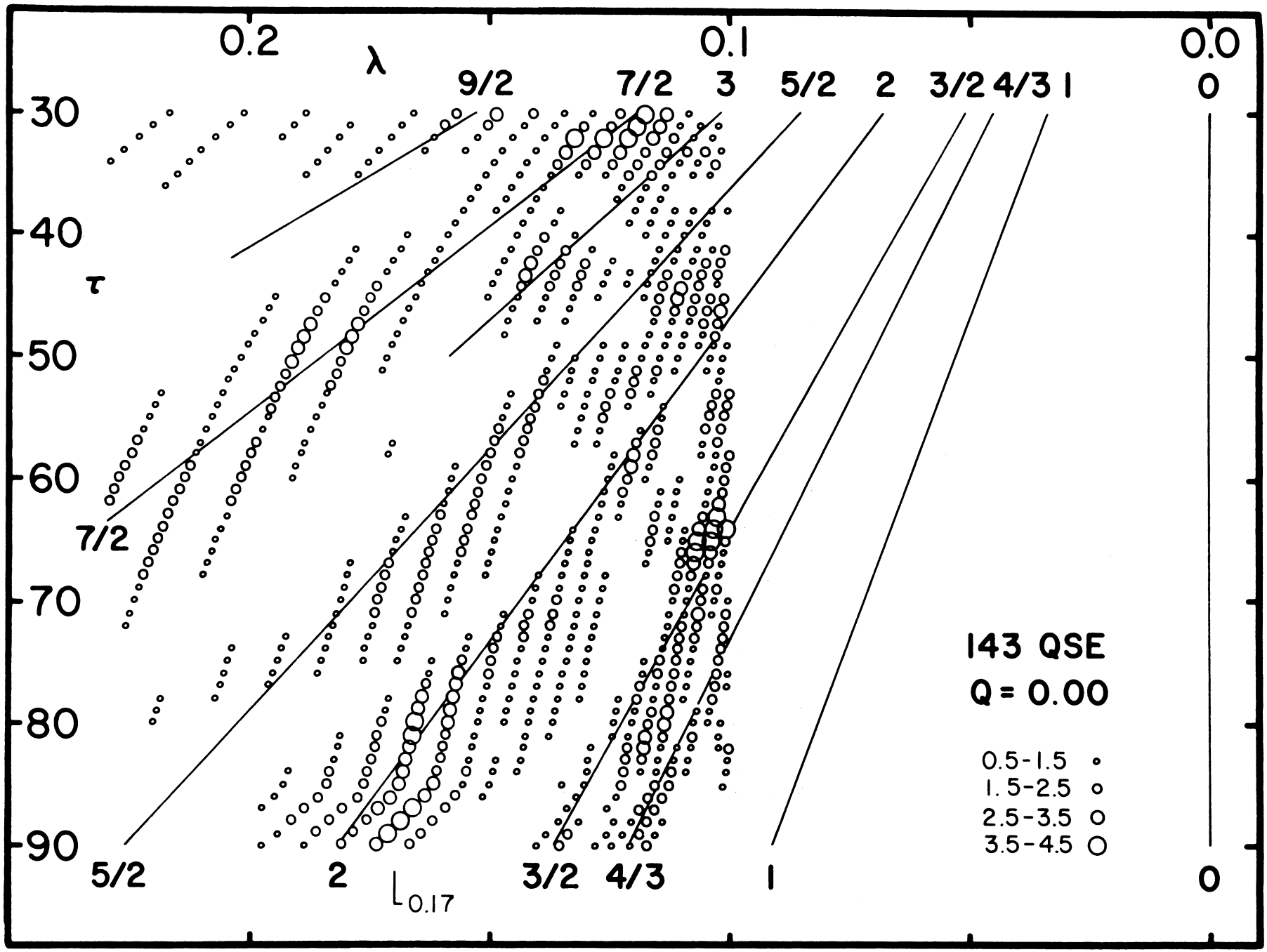
0.2
λ
0.1
0.0
9/2
7/2
3
5/2
2
3/2
4/3
1
0
30
40
τ
50
60
7/2
70
80
90
5/2
2
3/2
4/3
1
0
L0.17
143 QSE
Q = 0.00
0.5-1.5
1.5-2.5
2.5-3.5
3.5-4.5

FIGURE 10

The wavelength, λ, of z'' power spectrum peaks as a function of projection angle, τ, for the 143 QSE sample at Q=0.00. Only the peak value of each peak exceeding 3.5 is shown. The peaks group about lines which are simple multipes of the primary band pattern frequency. The 0.07 and 0.06 periodicities which have been observed in QSS z distributions can be identified with the X3/4 and X2/3 multiples of the primary band wavelength at $\tau=90^{o}$. Some of the short wavelength peaks for τ near 75^{o}, s=8.5 may result from substructure within the bands themselves.

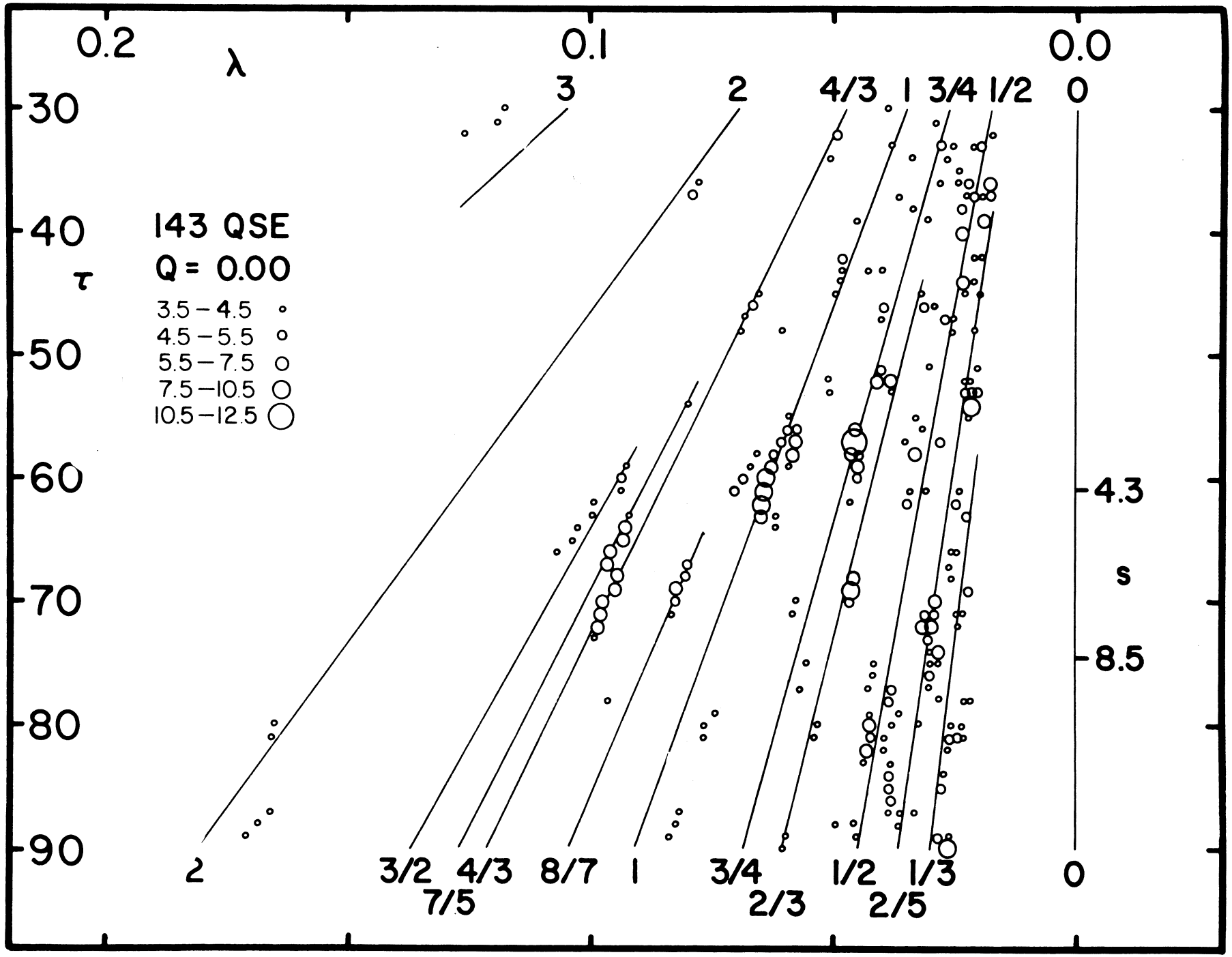
0.2
λ
0.1
0.0
3
2
4/3
1
3/4
1/2
0
30
40
τ
50
60
70
80
90
143 QSE
Q = 0.00
3.5 – 4.5
4.5 – 5.5
5.5 – 7.5
7.5 – 10.5
10.5 – 12.5
4.3
s
8.5
2
3/2
7/5
4/3
8/7
1
3/4
2/3
1/2
2/5
1/3
0

FIGURE 11

The wavelength, λ, of z'' power spectrum peaks as a function of projection angle, τ, for the 143 QSE sample at Q=0.02. The figure is the same as figure 10 excepting for Q. Near Q=0.02 maximum suppression of the main peak occurs.

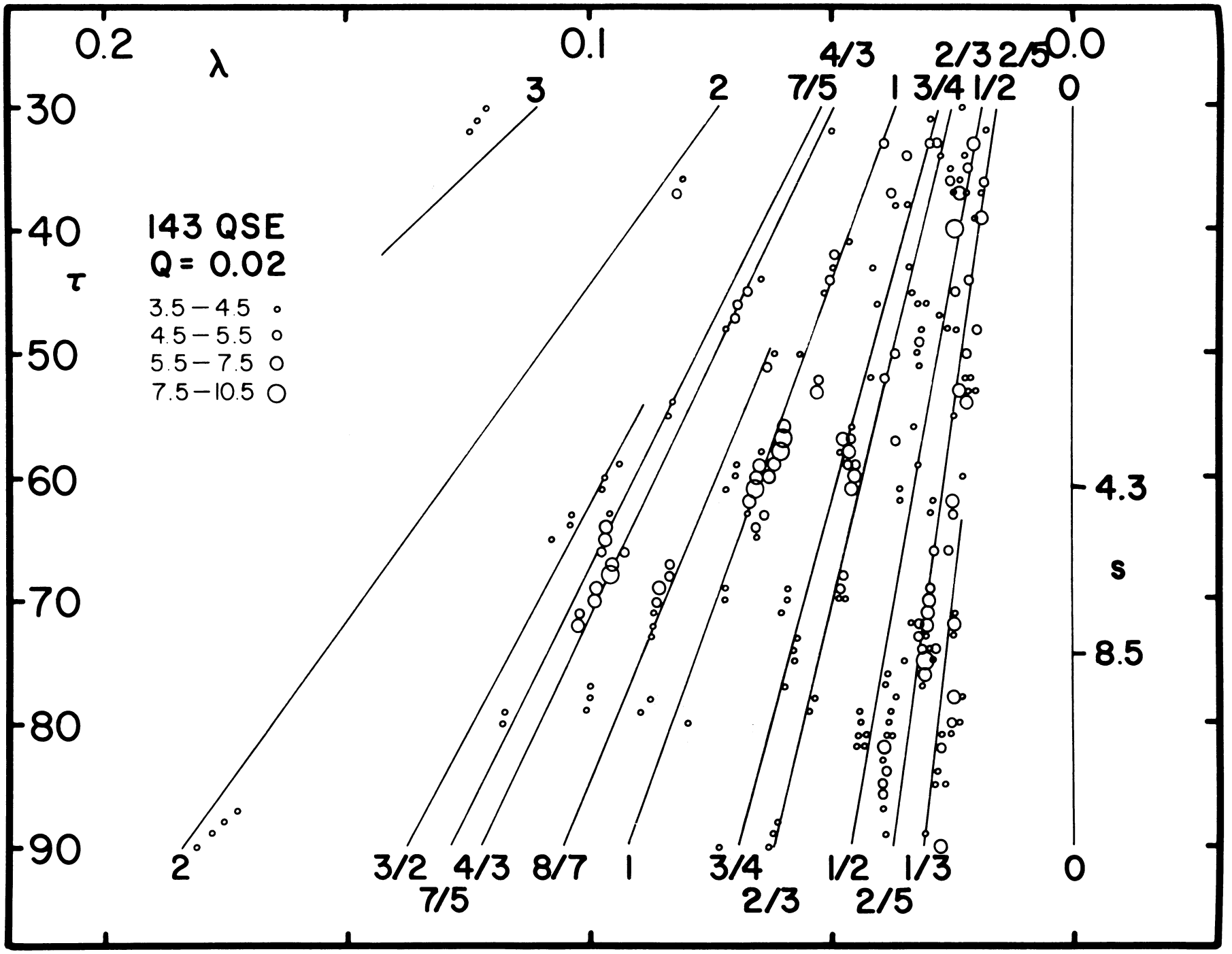
0.2
λ
0.1
0.0
4/3
2/3
2/5
3
2
7/5
1
3/4
1/2
0
30
40
τ
50
60
70
80
90
143 QSE
Q = 0.02
3.5 – 4.5
4.5 – 5.5
5.5 – 7.5
7.5 – 10.5
4.3
s
8.5
2
3/2
7/5
4/3
8/7
1
3/4
2/3
1/2
2/5
1/3
0

FIGURE 12

The wavelength, λ, of z'' power spectrum peaks as a function of projection angle, τ, for the 143 QSE sample at Q=0.08. The figure is the same as figure 10 excepting for Q. Near Q=0.08 maximum enhancement of the main peak occurs.

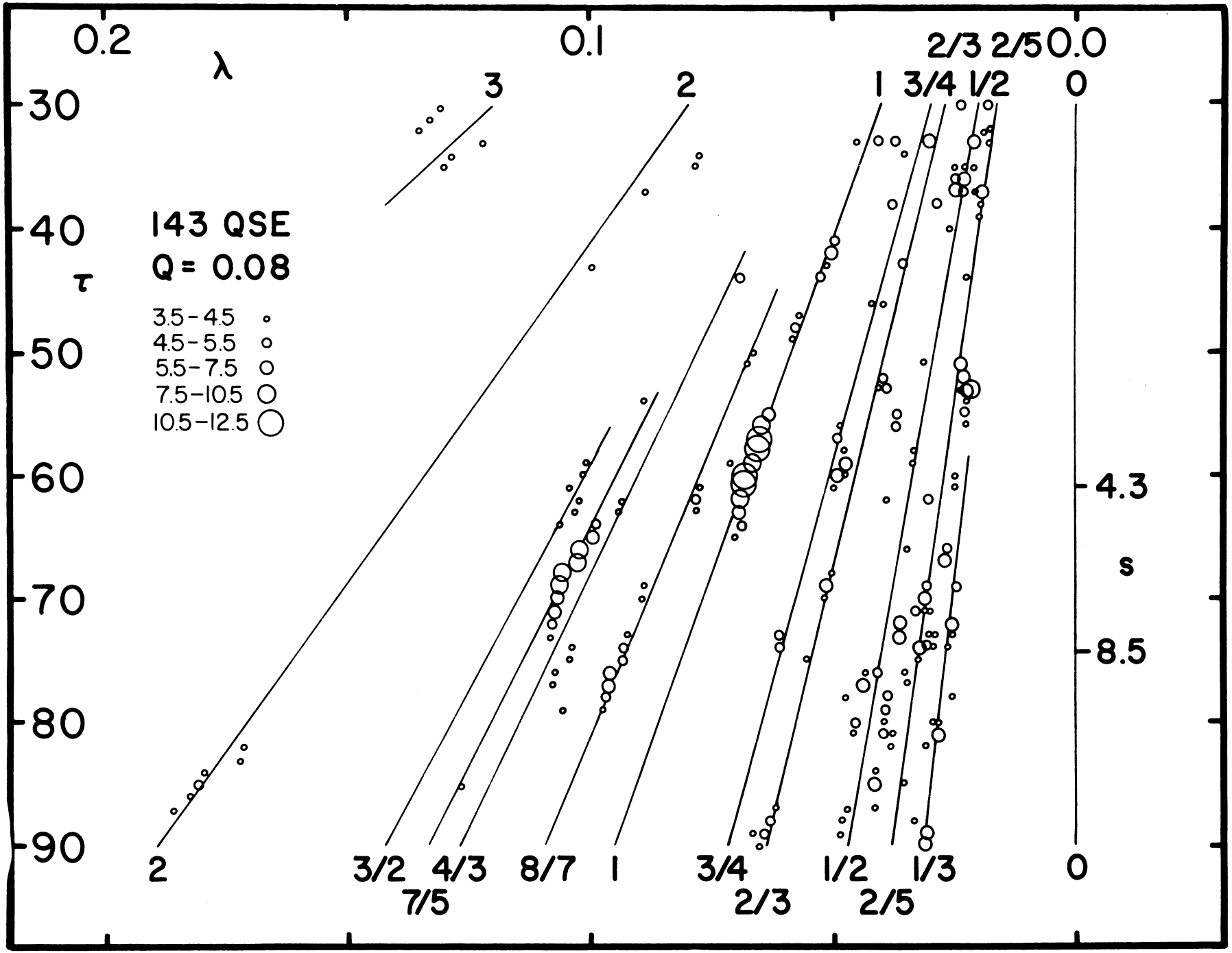
0.2
λ
0.1
2/3 2/5 0.0
3
2
1 3/4 1/2
0
30
40
τ
50
60
70
80
90
143 QSE
Q = 0.08
3.5-4.5
4.5-5.5
5.5-7.5
7.5-10.5
10.5-12.5
4.3
s
8.5
2
3/2
4/3
8/7
1
3/4
1/2
1/3
0
7/5
2/3
2/5

THE RELATIONSHIP OF THE QSE BAND SYSTEM TO THE COMA BAND SYSTEM

In figure 13 the QSE band system has been shifted by -1.24 in logz and -2.00 in magnitude and superimposed upon the total magnitude band system of Coma. Galaxies assigned to the odd and even bands are shown separately for clarity. Band membership is assigned as in CII from V(4.8) photometry since the scatter in total magnitudes makes the band system difficult to see directly. The least squares fits from CII for the three major bands are shown with dashed lines. The fit is obviously very good; the Coma band system is a scaled version of the QSE band system. The equation for the relationship between the band systems is

$$\Delta(\log z) = X + \frac{.301}{s}\Delta m. \qquad (18)$$

The band systems are shifted by X in logz at constant magnitude to bring them into register and then shifted along the band slope until the individual object points register. To go from the QSE to the Coma band systems, X=-1.10 and Δm=-2.00. The band systems are not only identical in slope, but also in the detailed character of their series convergence. Thus, the answer to the QSS test hypothesis stated earlier is yes in all respects.

The agreement between the systems may extend beyond the band slope and spacings and apply to the distribution of points within the bands. In figure 13 two characteristic features in the galaxy distribution along the bands are indicated. The same features were indicated in figure 6 for the QSE band system. In figure 14 the galaxy and QSS points are shown superimposed. The similarity in their distribution offers further support for the reality of the spin group substructure discussed in CII.

The total magnitudes assumed for Coma galaxies in this paper are 0.2 magnitudes brighter than given by Rood (1969) and used in CII. The reason for this slight shift is the presence of a small systematic error in the photometric calibration of Rood and Baum (1968) as shown by Ables and Ables (1972). In a study of the Coma cluster galaxy, NGC4881, Ables (1972) derived a revised total magnitude 0.2 magnitudes brighter than Rood (1969). Studies in progress indicate that when the Ables and Ables (1972) intensity calibration correction is applied to other Coma cluster galaxies, they will brighten in a similar way, hence, the 0.2 magnitude correction has been applied to all the galaxies.

FIGURE 13

The QSE band system superimposed upon the Coma cluster total visual magnitude-logz diagram after shifting by constants given in the text. Coma galaxies associated with the odd numbered bands are shown on the left and those associated with even numbered bands are shown on the right. Heavy dashed lines are the CII least squares fits to the Coma total magnitude bands. The light dashed lines indicate the galaxy groups used in fitting between systems. Within the accuracy of the data the Coma band system is a scaled version of the QSE band system.

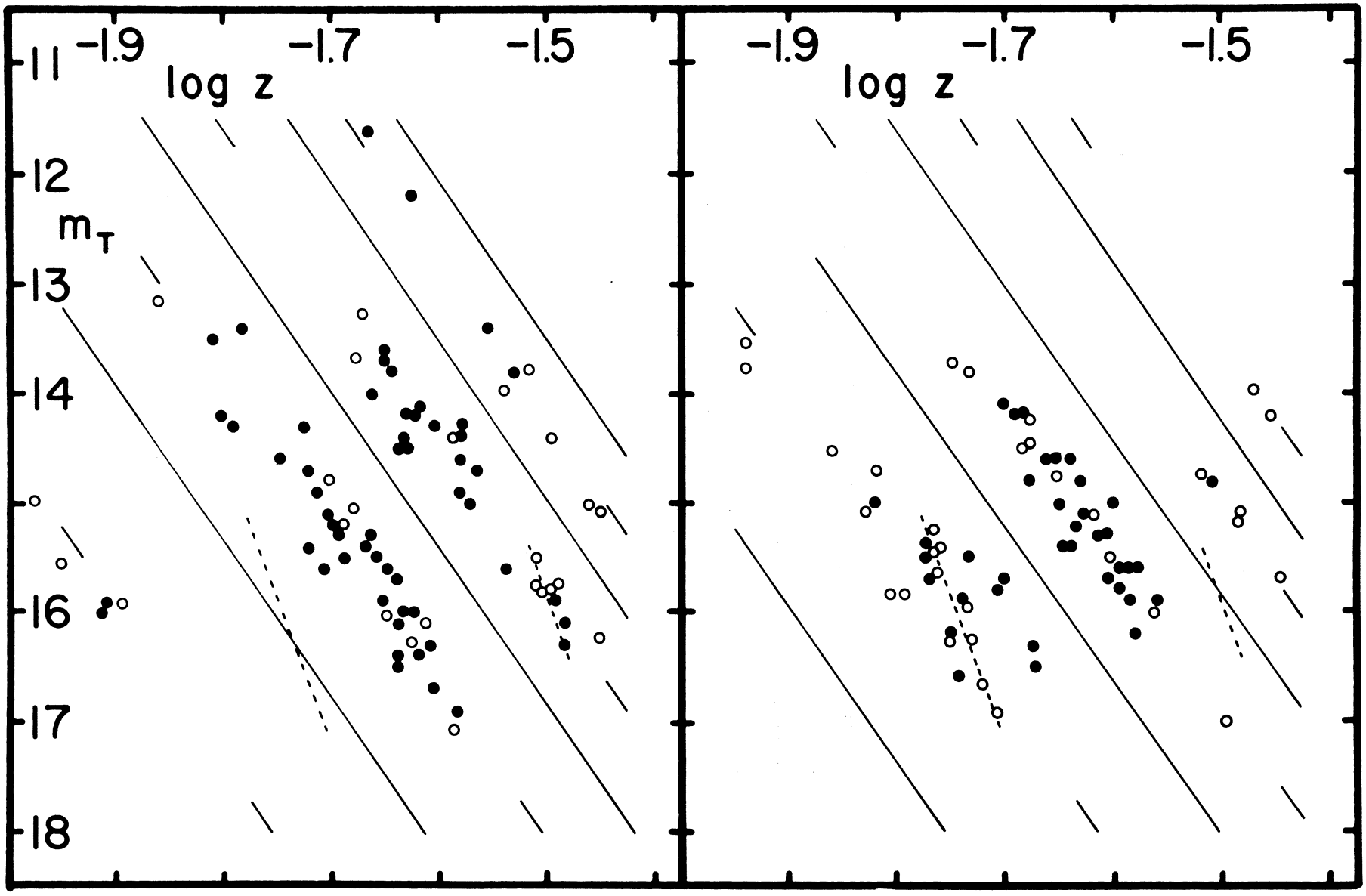

Figure 14

FIGURE 14

The QSE band system superimposed upon the Coma cluster total visual magnitude-logz diagram after shifting by constants given in the text. The figure is organized as in figure 13 with odd band populations on the left and even band objects on the right. Galaxies are shown with filled circles and QSS objects with open circles.

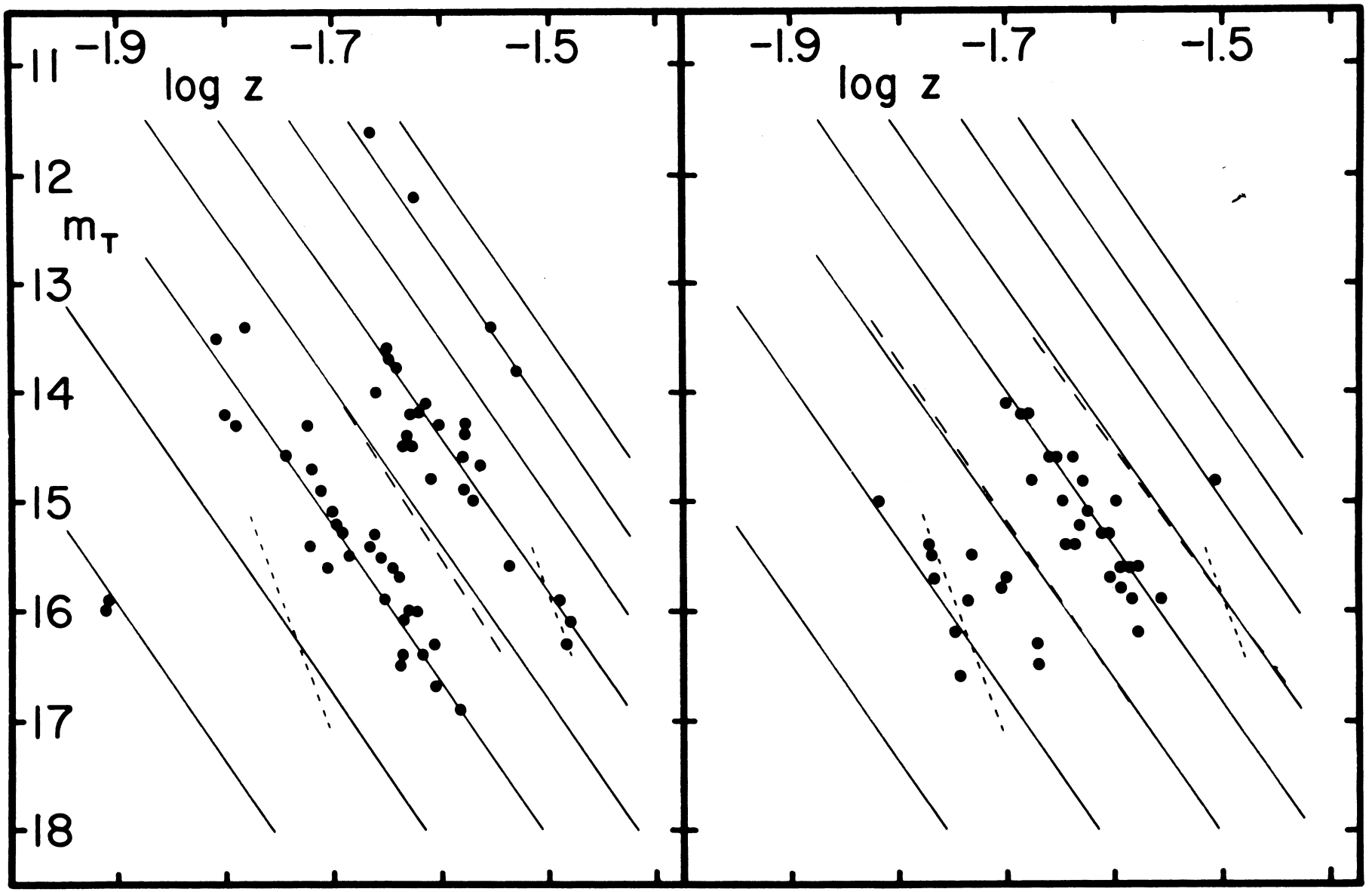

Figure 13

THE E BAND SYSTEM

The QSE objects appear to form a comprehensive band system. The Coma system is obviously not a part of the QSE system since it forms an independent convergent series. One can, therefore, hypothesize that the Coma cluster band system forms part of a comprehensive galaxy band system. We shall refer to the galaxy system, including Coma, as the E band system since it will be seen to be characterized by clusters which are dominated by elliptical galaxies. Very few total visual magnitudes equivalent to those in the Coma cluster exist for galaxies. Magnitudes for approximately 80 of the brightest galaxies in clusters have been published in the form of a Hubble diagram by Sandage, et. al. (1972), however, individual data is not given. McVittie (1972) has published magnitudes and z values for about half of the 80 objects derived by measurement from published graphs. This same procedure has been applied to the Hubble diagram published by Sandage, et. al. (1972). A comparison of the magnitudes and redshifts measured from Sandage, et. al. (1972) with McVittie (1972) shows excellent agreement in nearly every case in common. Only certain general characteristics of the redshift-magnitude diagram are required in this paper and there are no references to specific objects or values.

Figure 15 is the comprehensive m-logz diagram for the E galaxy system. The distribution of bright galaxies forms an upper envelope at the Hubble slope 5; the Coma band system lines intersect the Hubble line at a steep angle. At the high redshift end the QSE band system is drawn; the two band systems are drawn identically except for the fitting shift previously discussed. Several important features appear in the diagram.

The distribution of bright galaxies is not uniform along the Hubble line. There may be a break or weakening near 30,000 km/sec followed by a distinct clumping between 40,000 and 60,000 km/sec. A sharp break then occurs with only a few scattered points recurring near 100,000 km/sec. The 60,000 km/sec break could be a selection effect but it is a remarkable coincidence that it occurs precisely where the first QSE band occurs. The few scattered points at higher redshift further match the second and third QSE system bands. It is, therefore, possible to suspect that the E band system forms a series which converges upon the first QSE band as its series limit.

In one respect the E band system differs from the QSE system. The E band system must contain more than 14 bands since if the QSE system is superimposed exactly band 14 falls at the dotted line in figure 15. A study

FIGURE 15

The E band system and its relationship to the QSE band system shown on the right. Coma cluster galaxies are shown with filled circles and even numbered band objects are omitted. QSS objects on the first QSE system band and others with V<15.5 are shown with open circles. Bright galaxies according to McVittie (1972) are shown with X symbols and those from Sandage, et. al. (1972) are shown with + symbols. An underline indicates objects which probably appear in duplicate. The standard Hubble line through the bright galaxies is shown. The most striking feature of the diagram is the association of the high z galaxies with the lower limit of the QSE band system.

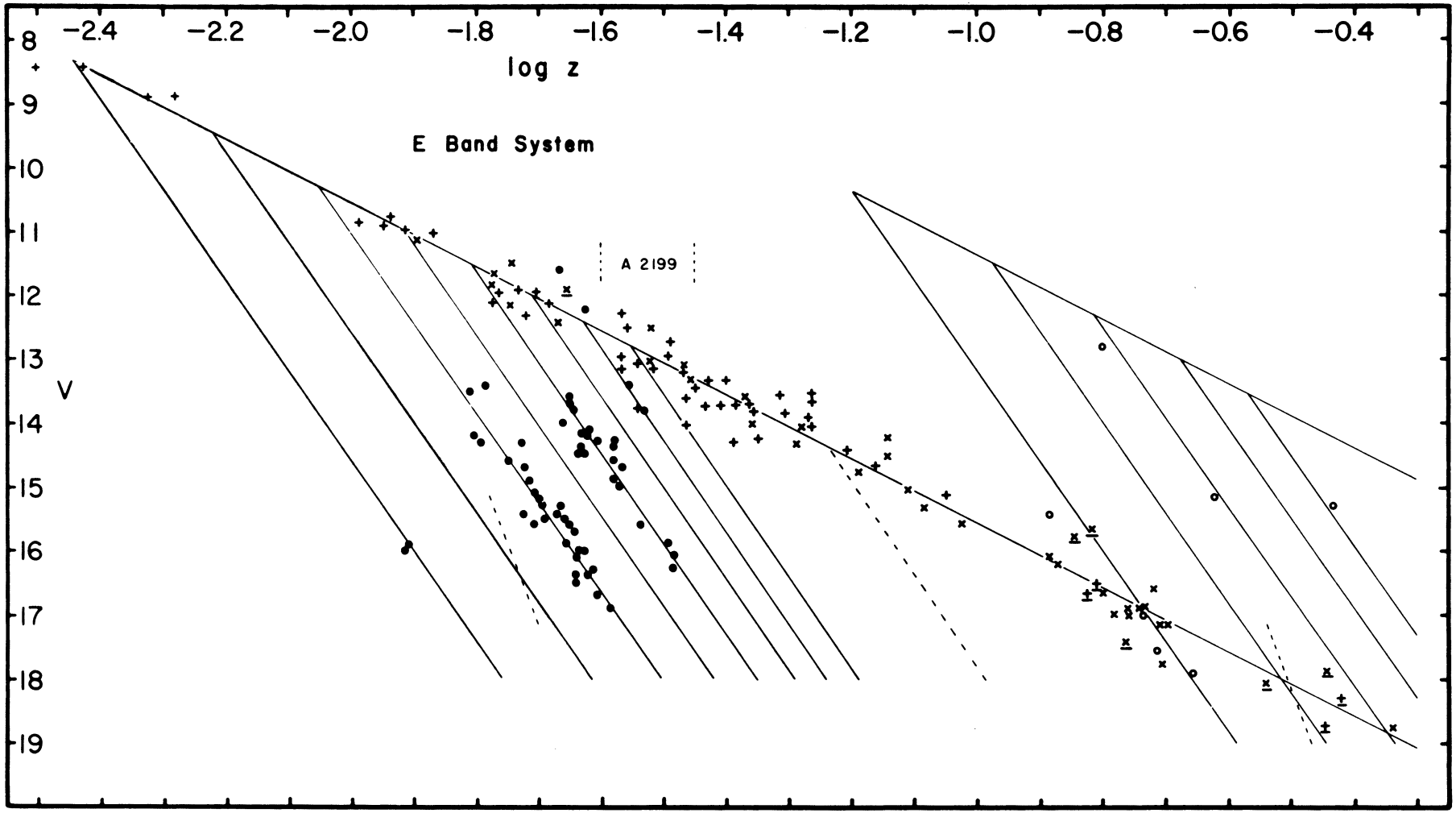
log z
−2.4
−2.2
−2.0
−1.8
−1.6
−1.4
−1.2
−1.0
−0.8
−0.6
−0.4
E Band System
A 2199
V
8
9
10
11
12
13
14
15
16
17
18
19

of the higher band structure will require investigation of a fairly large number of high redshift clusters. Above the Hubble line an interval is indicated within which the A2199 cluster falls. A preliminary study of this cluster (Tifft, 1972b) shows bands more closely spaced than the Coma cluster consistent with the convergent series. Extension of studies through a wide range of redshift is obviously required.

One final feature of the QSE band system can now be recognized by comparison with the E system. The QSE system has an upper magnitude bound with the standard Hubble line slope of 5 within the limits of the data sample. The upper magnitude limit in figures 6 and 15 has been drawn with the same fitting shifts as other parts of the diagram and it is seen to pass just above 3C 273 and all but one of the higher redshift QSE objects up through band 14.

THE QSA BAND SYSTEM

In figure 16 we examine the upper redshift limit of the QSE band system. It has already been noted in figure 1 that a break in frequency of QSE objects occurs at band 14. Beyond this limit QSA objects become common. Furthermore, the QSA objects show little regard for the QSE Hubble line upper bound. If in analogy with the E-QSE interface we take band 14 as a series limit and superimpose a new band system beginning at that point, we find that within the limits of small numbers of objects the QSA objects fit an independent band system, the QSA system, of identical slopes, spacings, and lower limit properties to the QSE system.

It is also possible to identify the characteristic grouping of points on the second band which has been identified and used for intersystem fitting. This feature can now be recognized as the grouping of the QSS objects near $z=1.95$. We also note that just as galaxies overlapped into the QSE system, QSE objects overlap into the QSA system but where they overlap they concentrate on the higher system's bands.

To complete the comparison of systems, we examine the upper magnitude bound of the QSA system. Markarian 132 has only an approximate magnitude but it has been added to figure 15. An upper Hubble line slope analogous to the other systems has been drawn above it. The fitting shifts to go from the QSE to the QSA systems according to equation 18 are $X=+0.845$, $\Delta m=+0.50$.

FIGURE 16

The QSA band system and its relationship to the QSE band system. Several higher bands and the Hubble line envelope of the QSE system are shown dashed. QSE objects are shown with filled circles and QSA objects with open circles. Markarian 132 is shown with a square. Just as the galaxies in figure 15 showed a break in frequency at the first QSE band with higher z galaxies falling on higher QSE bands, the QSE objects show a frequency break at the first QSA band and higher z objects concentrate on the higher QSA bands. The n=2 feature shown lightly dashed is the feature used for intersystem fitting and can here be associated with the z=1.95 concentration of redshifts.

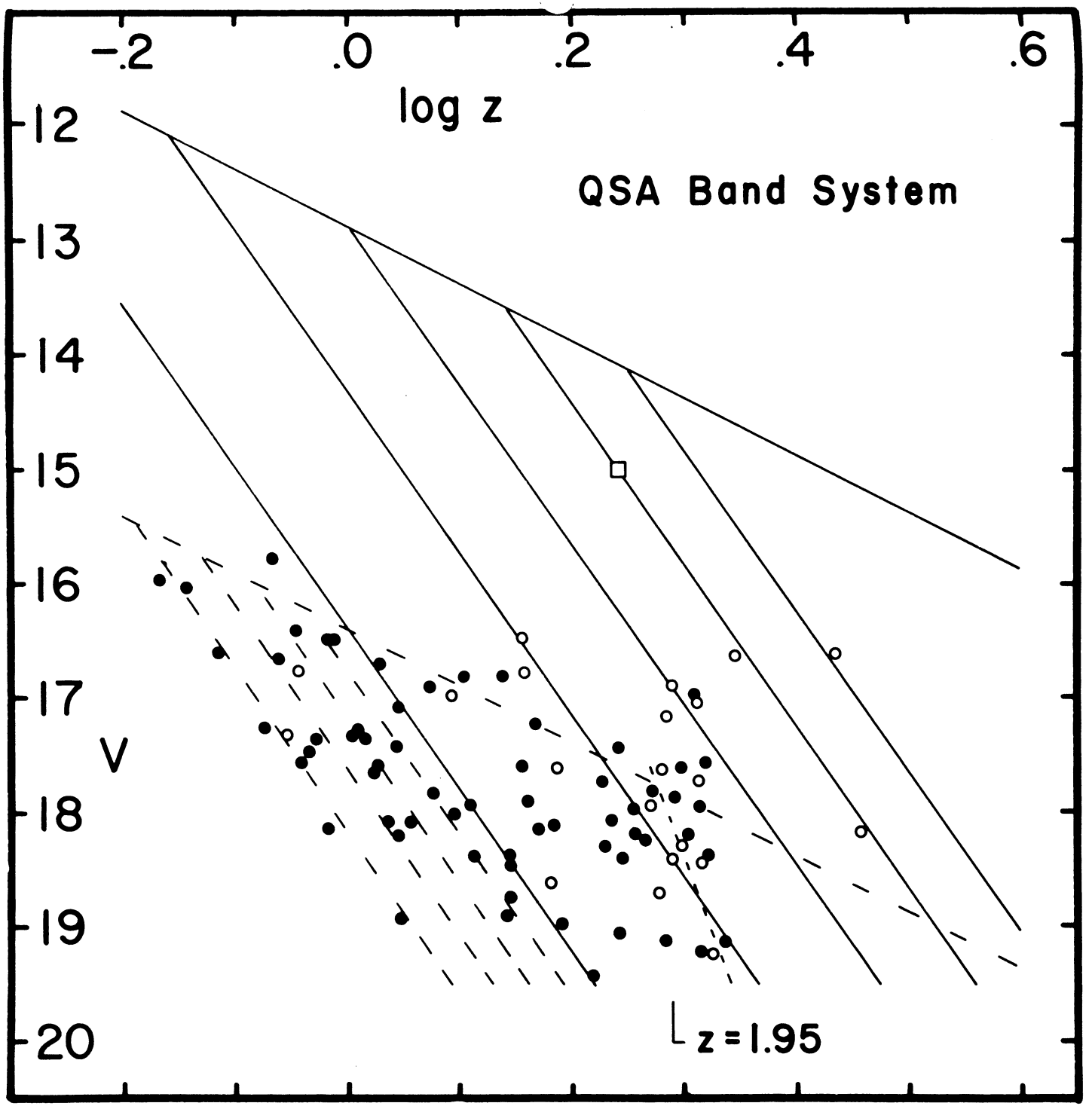
-.2
.0
.2
.4
.6
log z
12
13
14
15
16
17
18
19
20
V
QSA Band System
z=1.95

SUMMARY

The reality of the redshift-magnitude band phenomenon rests upon the following observations.

A. The investigations of the Coma cluster, including:
   1. The statistical significance of the redshift-magnitude bands.
   2. The statistical significance of the redshift-magnitude-morphology (or ellipticity) correlation.
   3. The identity of direction of the above two effects.
   4. The Gaussian distribution of points about the bands.

B. The investigations of the QSE band system, including:
   1. The statistical significance of the m-logz banded relationship.
   2. The identity of the band slope with the Coma galaxies.
   3. The identity of the band spacing properties such that the E band system is a scaled version of the QSE band system.
   4. The fact that the band system forms a smoothly convergent series.
   5. The Gaussian distribution of points about the bands.
   6. The existence of the system provides an explanation of previously observed z periodicities in QSS objects.

C. Other factors, including:
   1. The boundary correlations between redshift systems including:
      a. The identity of the convergent limit of any system with the first band of the next higher system.
      b. The detailed relationship of bright galaxies to the boundaries of the E band system.
      c. Objects overlapping into a higher system conform to the bands of the higher system.
   2. A consistent rational or explanation for most discordant redshift phenomena including:
      a. Virial Theorem discrepancies.
      b. Discordant redshifts in small groups and redshift trends with magnitude within groups.
      c. The dependence of redshift on morphology within clusters.
   3. The observed band system in the A2199 cluster.
   4. A possible explanation of the z=1.95 concentration of objects.

DISCUSSION

If the band phenomenon is real, one conclusion appears inescapable; in

one form or another there must be multiple states or conditions of matter. The conceptual resemblance of the bands to excitation levels and the systems to ionization states, or some equivalent analogy, is apparent. The fundamental substructure of matter must be involved. The only discussion relating to such effects in the astronomical literature known to the author is a paper by Cowan (1968) where variable charge screening is considered as a mechanism to scale atomic energy levels in discreet steps. It would appear profitable to pursue such effects in more detail.

The second basic requisite appears to be come form of rapid evolution in galaxies. If this were not the case, even if galaxies are made of matter in different states, galaxies of all types should be seen over a wide range of distances and it is difficult to conceive of any mechanism to produce bands. Bands will appear, however, and the upper envelope will satisfy the Hubble law if we have the following conditions.

1. All objects have a common origin in time such that a given distance (lookback) shell represents a unique era in the history of the Universe.
2. All objects within a single band system evolve in luminosity, brightening with time until they reach a standard absolute luminosity. Beyond this point in time they rapidly dissipate leaving perhaps only a dwarf remnant. The luminosity limit may be different in different band systems.
3. The rate of evolution depends upon the state of matter (band index n) with higher states evolving proportionally faster. The rate presumably also depends upon some variable within an individual band population such that objects will disperse along the band.
4. A condition that redshift also depends upon time as discussed later.

With these conditions, at a given redshift and distance (specific earlier era of the Universe), galaxies of one particular matter state will have a particular luminosity and galaxies from other states will be brighter and fainter by discreet amounts. As we decrease the distance (later era) the luminosities will move up until as each point reaches the upper luminosity limit it dissipates. The distance variation effect on the standard absolute luminosity upper limit produce the apparent luminosity variation of the upper bound required by the Hubble law.

Without the fourth condition on redshift, each characteristic state of matter could have a different characteristic intrinsic redshift but pure luminosity evolution in the galaxies could not change it and evolutionary tracks would be vertical bands in the redshift magnitude diagram. In order to tilt the bands we must vary the redshift in some manner in step with the luminosity evolution so that at any given era a particular galaxy will have both luminosity and redshift specified. So long as we impose the condition that galaxies in a cluster are at the same distance there appear to be only three options available.

4a. The galaxy adds some redshift component to the basic intrinsic component which varies systematically during its evolution.

4b. In the course of luminosity evolution, different substates of matter are sequentially presented to provide a sequence of intrinsic redshifts. The individual substates need not have time dependent properties.

4c. The properties of matter or energy themselves are time dependent.

Condition 1 is the normal condition for a singular origin Universe. Parts of conditions 2 and 3 have some theoretical basis in the origin and evolution of galaxies by expansion from dense cores as has been discussed by Harrison (1970). It is of interest that angular momentum is a discriminant on rate of evolution according to Harrison (1970), and it does appear to vary along the Coma cluster bands.

Condition 4a requires a mechanism much as gravitational redshifts, however, large gravitational redshifts have been shown to be untenable because of the blurring effect on the spectrum (Wolfe and Burbidge, 1970) and no other mechanism appears feasible. A theoretical basis for 4c has been provided by Hoyle and Narlikar (1972).

One quantity that has not been discussed to any extent so far is distance and how distance varies with z. This question will be considered in a separate paper, however, some general commentary is possible. It seems fairly plausible that within a single band system distance varies with z. Arguments in support of this include the Hubble law and the observation given in this paper where the magnitude dispersion about the bands in the QSE system is shown to decrease with n. It is less obvious that the relationship of distance to z extends smoothly across redshift system boundaries. The potential impact of this possibility on the interpretation of QSS distances is of particular interest, however, it is premature to pursue the concept too far at this time.

REFERENCES

Ables, H. D., and Ables, P. G. 1972, AAS Photo. Bull., in press.

Ables, H. D. 1972, A.J., in press.

Cowan, C. L. 1968, Ap.J. (Letters) 154, L5.

DeVeny, J. B., Osborn, W. H., and Janes, K. 1971, P.A.S.P. 83, 611.

Harrison, E. R. 1970, M.N.R.A.S. 148, 119.

Hoyle, F., and Narlikar, J. V. 1972, M.N.R.A.S. 155, 305 and 323.

Lake, R. G., and Roeder, R. D. 1972, J.R.A.S.C. 66, 111.

Lynds, R., and Wills, D. 1972, Ap.J. 172, 531.

McVittie, G. C. 1972, M.N.R.A.S. 155, 425.

Rood, H. J. 1969, Ap.J. 158, 657.

Rood, H. J., and Baum, W. A. 1967, A.J. 72, 398.

_____. 1968, ibid, 73, 442.

Sandage, A., Tamman, G. A., and Hardy, E. 1972, Ap.J. 172, 253.

Tifft, W. G. 1972a, Ap.J. 175, 613.

_____. 1972b, Steward Observatory Preprint No. 45.

_____. 1973, Ap.J. 179, Jan. 1, 1973, in press.

Wolfe, A. M., and Burbidge, G. R. 1970, Ap.J. 161, 419.

Yu, J. T., and Peebles, P. J. E. 1969, Ap.J. 158, 103.